THE ASTROPHYSICAL JOURNAL, 408:262–276, 1993 May 1

THE $^6Li/^7Li$ RATIO IN THE METAL-POOR HALO DWARFS HD 19445 AND HD 84937

VERNE V. SMITH,[1] DAVID L. LAMBERT,[1] AND POUL E. NISSEN[1,2]

Received 1992 September 2; accepted 1992 October 26

ABSTRACT

High-resolution high signal-to-noise spectra of the Li I 6707 Å line in the subdwarfs HD 19445 and HD 84937 have been analyzed for the presence of ^6Li. By measurement of the Li I lines's wavelength and analysis of its profile, the atmosphere of HD 84937 is shown to have a small amount of ^6Li: $R = {}^6Li/Li = 0.05 \pm 0.02$. For HD 19445, an upper limit is set of $R < 0.02$. The presence of ^6Li in HD 84937 is consistent with the mild depletion of ^6Li predicted by standard (nonrotating) models and the initial presence of ^6Li in the halo produced by (principally) α-on-α fusion reactions involving the cosmic rays that are required to account for the Be and B observed in subdwarfs. Depletion of ^6Li in the lower mass star HD 19445 is expected to remove the initial ^6Li content and, hence, the absence of ^6Li is expected. If Yale models of rotating subdwarfs are adopted, the predicted severe depletion of ^6Li and the observed survival of ^6Li in HD 84937 have to be reconciled. Four suggestions are made: the rotating models are inapplicable to halo dwarfs, production of ^6Li by cosmic rays has been underestimated, the required high initial ^6Li abundance of the halo was produced prior to the formation of the Galaxy, or the ^6Li was produced in stellar flares.

Subject headings: nuclear reactions, nucleosynthesis, abundances — stars: abundances — stars: individual (HD 19445, HD 84937) — stars: Population II

1. INTRODUCTION

Spite & Spite's (1982) detection of lithium in halo dwarf stars initiated the use of this fragile trace element as a probe of the nucleosynthesis achieved during the big bang. Unfortunately, this probe is not as incisive as, perhaps, hoped immediately following its initial use. One primary source of uncertainty is the possibility that the surface lithium abundance is now less than at a star's birth: destruction of Li by protons at $T > 2 \times 10^6$ K, as well as a diffusive loss of Li, are distinct possibilities. These effects would cause the observed Li abundance in the halo dwarfs to be a lower limit to the star's initial Li abundance, which has often been identified as the big bang abundance. Recently Steigman & Walker (1992) point out that Li synthesized in the early Galactic halo by cosmic rays through α on α fusion reactions may supplement the pre-Galactic or big bang Li abundance.

Lithium abundances of the halo dwarfs are independent of metallicity for [Fe/H] < -1.0 and of effective temperature for $T_{\rm eff} \gtrsim 5600$ K. This abundance, referred to here as the "plateau" abundance, is $\log \epsilon(\rm Li) = 2.17$ (Deliyannis, Demarque, & Kawaler 1990) on the scale where $\log \epsilon(\rm H) = 12.00$. In this paper, we present an attempt to measure the abundance ratio of the two stable isotopes of lithium, ^6Li and ^7Li, in two halo dwarfs having the plateau Li abundance. Our observations provide the first detection of ^6Li in a subdwarf and a stringent upper limit to the $^6Li/^7Li$ ratio in a second star. Both the detection and the upper limit are less than previously reported upper limits of $^6Li/^7Li \lesssim 0.1$ for subdwarfs (Maurice, Spite, & Spite 1984; Pilachowski, Hobbs, & DeYoung 1989).

By combining an observed $^6Li/^7Li$ ratio with theoretical astration rates of ^6Li and ^7Li, one infers a star's initial $^6Li/^7Li$ ratio, i.e., the ratio present in the halo gas from which the star formed. The initial $^6Li/^7Li$ ratio may then be compared with that predicted for the combined products of a big bang and of synthesis by the cosmic rays that are believed to have been responsible for the Be and B observed in the stars for which the $^6Li/^7Li$ ratio has been measured.

Astration (i.e., destruction) of Li within a star is achieved by protons at temperatures greater than about 2×10^6 K. At a given temperature, ^6Li is destroyed more quickly than ^7Li. If the surface convection zone extends at any time to layers hotter than about 2×10^6 K, the surface Li abundance will be depleted and the $^6Li/^7Li$ ratio reduced. Although, as we emphasize in § 4, predictions of the degree of astration remain uncertain, it does appear that the astration is least severe in the most massive of the subdwarfs (Brown & Schramm 1988; Deliyannis et al. 1990; Deliyannis 1990; Pinsonneault, Deliyannis, & Demarque 1992). Therefore, a search for ^6Li in a subdwarf is most likely to be successful in those of the highest effective temperature, i.e., at the main-sequence turnoff for the halo population. In our attempt to detect surviving ^6Li we elected to examine HD 84937, a star also identified as a promising candidate by Brown & Schramm (1988). As a control star expected to have no detectable surviving ^6Li, we examined HD 19445.

2. OBSERVATIONS AND DATA ANALYSIS

2.1. *Observation Log and Data Reduction*

Spectra of the region containing the Li I 6707 Å resonance doublet were obtained for HD 19445 and HD 84937 with the McDonald Observatory's 2.7 m reflector and coudé spectrometer with a Tektronix 512 × 512 CCD. An echelle grating was used which, with the 27 μm square size of the CCD pixels, yielded a scale at the CCD of 0.0265 Å pixel^{-1} (0.981 Å mm^{-1}): the spectral coverage across the CCD was thus about 13.5 Å.

The stars were observed on the nights of 1991 December 12/13 and 13/14. Four 40 minute integrations were obtained on HD 19445 and eight 60 minute integrations on HD 84937: we list in Table 1 the observations for both stars along with the signal-to-noise ratios (S/N) for the individual spectra, as well as

[1] Department of Astronomy and McDonald Observatory, University of Texas, Austin, TX 78712.
[2] Institute of Physics and Astronomy, University of Aarhus, DK 8000 Aarhus C, Denmark.

TABLE 1

PROGRAM STAR OBSERVATIONAL DATA

STAR	McDONALD OBSERVATION NUMBER	S/N	EQUIVALENT WIDTHS (mÅ) Li I λ6707	Ca I λ6717
HD 19445.....	1	141	36.8	10.3
	2	112	35.8	12.2
	3	115	35.0	10.7
	4	130	33.9	9.9
HD 84937.....	10	140	26.0	7.8
	11	145	25.3	6.0
	12	150	26.3	6.8
	13	155	25.0	7.1
	48	143	23.5	5.7
	49	130	24.2	6.5
	50	147	25.0	5.8
	51	122	27.3	6.6

equivalent widths for the Li I (6707.8 Å) and Ca I (6717.7 Å) lines visible in this spectral region. On the second night, when the last four frames of HD 84937 were obtained, the grating tilt was changed slightly in order to place the Li I and Ca I lines on different parts of the CCD. The spectra were reduced using the routines in IRAF with bias subtraction done using a series of bias frames obtained on the same night and flat-fielding done using both a quartz lamp located just in front of the entrance slit, as well as a rapidly rotating hot star. No significant detectable differences were found between using the quartz lamp or the hot star, and fringing in this CCD is negligible. In Figures 1 and 2, we illustrate the combined final spectra for HD 19445 and HD 84937, respectively. The Li doublet, as well as the Ca I 6717.681 Å line, are clearly visible in both stars: combined S/N ratios are 240 for HD 19445 and 390 for HD 84937.

In addition to the spectra containing the Li I 6707 Å doublet and Ca I 6717 Å line, the Ca I 6162 Å line was observed with the same spectrometer. For the Ca I 6162 Å region, a TI 800 × 800 CCD with 15 μm square pixels was used which gave a scale of 0.0139 Å pixel^{-1} (0.927 Å mm^{-1}) on the CCD at 6162 Å. Fits to the Th hollow-cathode lines indicated a full

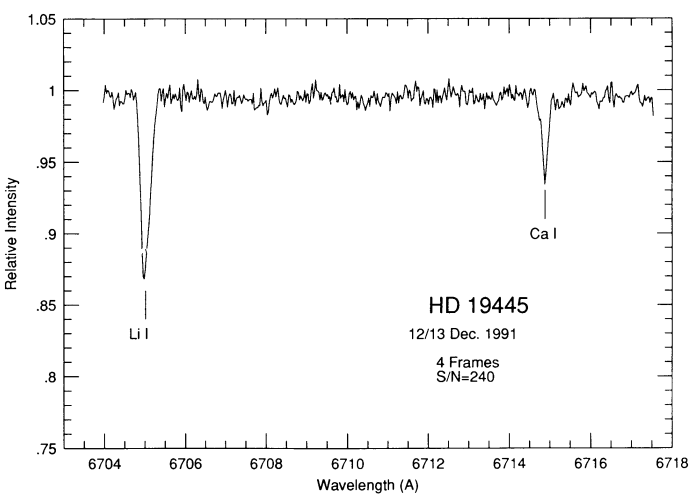

FIG. 1.—Average spectrum of HD 19445 with the Li I and Ca I lines indicated. This is a combination of four individual frames with a combined S/N ratio, in the continuum, of about 240. The wavelength scale is set by the Th lines and the stellar spectrum has not been shifted, illustrating the stellar radial velocity.

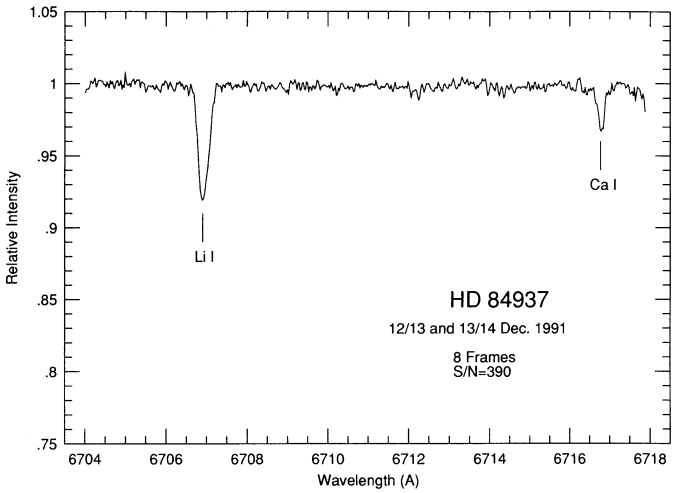

FIG. 2.—Average spectrum of HD 84937 showing the Li I and Ca I lines, which are weaker than in HD 19445 due to the 200 K hotter $T_{\rm eff}$ of HD 84937. This combined spectrum is the result of eight frames taken over two nights, with the individual spectra shifted onto a common wavelength scale: the final continuum S/N is about 390. The wavelength scale is set by the Th lines and the radial velocity shift of HD 84937 is evident.

width at half-maximum of just greater than 3.3 ± 0.1 pixels, or a resolution 0.0464 Å and R = 132,800. The stronger and well-defined Ca I 6162 Å line is used to determine the intrinsic stellar broadening in both HD 19445 and HD 84937. In both stars, it is found that the stellar broadening is greater than the spectrometer resolution (~5–6 km s^{-1} vs. ~2.2–2.4 km s^{-1}, respectively), thus, the stellar line profiles are dominated by the stellar broadening and not the spectrometer resolution. The Ca I 6162 Å spectra were obtained on 1991 December 27/28 and the S/N's are 143 and 135 for HD 19445 and HD 84937, respectively.

2.2. *How Accurate Are the Wavelengths*

The absolute wavelength calibration is important for the analysis of the Li I line profile, as well as its wavelength with respect to the nearby Ca I 6717.681 Å line. The wavelength calibration was set by Th-A hollow cathode lamp and, over this spectral interval, some eight Th lines were used for the calibration. We list these lines in Table 2: the wavelengths have been taken from Palmer & Engleman (1983). The entrance slit to the spectrometer was set at a projected width on the CCD of 67 microns, or 2.3 pixels (the measurements of the full width at half-maximum (FWHM) of the Th lines yielded a mean of 2.1 ± 0.1 pixels, or a resolution of 0.0538 Å, with no change in focus across the CCD: this yields a resolution R = 124,000). A

TABLE 2

THORIUM LINES USED IN THE WAVELENGTH CALIBRATION

Wavelength (Å)[a]	Intensity
6704.0510.....	2.5
6708.8411.....	0.8
6711.2521.....	8.1
6713.5972.....	1.0
6715.1885.....	1.6
6715.5136.....	1.4
6717.3851.....	8.0

[a] From Palmer & Engleman 1983.

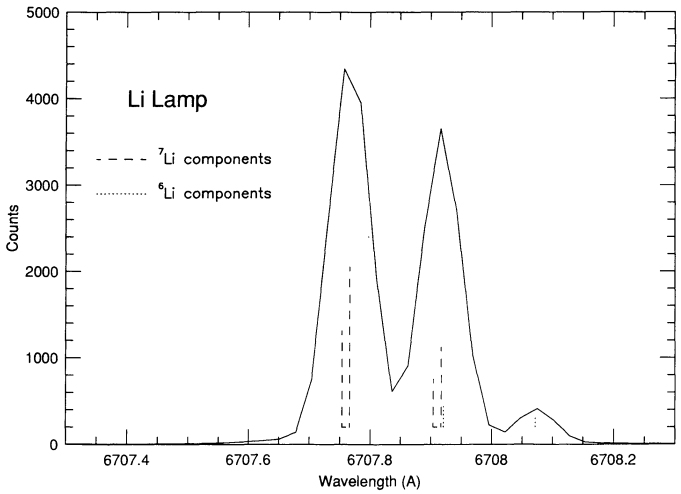

FIG. 3.—Illustration of the Li hollow-cathode lamp as observed by the coudé spectrometer. The ^{7}Li doublet is separated cleanly, while the red ^{6}Li line is evident. Vertical lines show the wavelengths of the various Li components, with the length of the line proportional to the *gf*-value and the abundance, assuming a ratio of ^{7}Li/^{6}Li = 12.3.

fit to the measured pixel positions of the Th lines to their wavelengths resulted in residuals between the measured positions and the fit of, at most, 0.005 Å. A comparison of Th spectra taken at the beginning and end of the night agreed to within 0.007 Å demonstrating that there was very little drift, if any, in the spectrometer wavelength calibration.

A simple test of the wavelength calibration is provided by a Li hollow cathode lamp, illustrated in Figure 3: the strong ^{7}Li doublet is visible, as is the redward, weaker ^{6}Li component. The first (bluest) component consists of the blended hyperfine components of the ^{7}Li 1/2–3/2 transition, while the second component consists of the ^{7}Li 1/2–1/2 hyperfine transitions plus the ^{6}Li 1/2–3/2 line. Finally, the reddest component is the ^{6}Li 1/2–1/2 transition. We list in Table 3 the wavelengths and *gf*-values of the Li components, taken from Andersen, Gustafsson, & Lambert (1984), while in Table 4 we list the calculated, blended wavelengths of the three components visible in our spectra of the Li I feature (Fig. 3), the observed wavelengths (using our Th calibration), and the (observed-calculated) wavelengths. The calculated wavelengths were computed by using an average of the wavelengths weighted by their respective *gf*-values and using a terrestrial mix for the ^{6}Li abundance (^{6}Li/^{7}Li = 0.08). As can be seen from Table 4, the Th comparison lines provide an accurate absolute wavelength scale, with very little drift, to within ±0.005 Å, to perhaps 0.007 Å over the course of the night.

TABLE 3

LITHIUM RESONANCE-LINE PARAMETERS

Isotope	J''–J'	F''–F'	λ(Å)	*gf*
^{7}Li.....	1/2–3/2	1–0, 1, 2	6707.754	0.371
		2–1, 2, 3	6707.766	0.618
^{7}Li.....	1/2–1/2	1–1, 2	6707.904	0.185
		2–1, 2	6707.917	0.309
^{6}Li.....	1/2–3/2	All	6707.921	0.989
^{6}Li.....	1/2–1/2	All	6708.072	0.494

2.3. *Measuring the Center-of-Gravity Wavelength of the* Li I *Feature*

This wavelength scale, with an internal accuracy of 0.005–0.007 Å, can be used to measure the wavelengths of both the Li I feature and the Ca I line in the program stars: as the Ca I wavelength is well-known and the center-of-gravity (cog) of the Li I feature depends upon the ^{6}Li fraction, the difference, Δ = Ca I–Li I, is a simple and straightforward way to characterize the Li I absorption. Each of the four frames of HD 19445 and eight of HD 84937 were measured for the wavelengths of the Li I and Ca I features and Δ calculated for each spectrum. The small dependence of this difference on radial velocity can be calculated: the other effect on the measured Δ's might arise from the differing line-strengths and excitation potentials of the resonance Li I doublet and the χ = 2.71 eV Ca I line. As the Ca I line is weaker than the Li I feature and arises from an excited level, it is formed deeper in the star's atmosphere and the measured wavelengths might be influenced slightly by convective velocities within the atmosphere.

The wavelengths were measured in each individual spectrum using the "splot" option in IRAF: for the Li I feature, the line was integrated numerically and the cog calculated. For Ca I, we assumed a single line and fit a Gaussian profile to the line: this provides a more accurate wavelength determination for this weak line that is less affected by noise. We present the results of the wavelength measurements of the Li I and Ca I lines in Table 5.

We discuss the measurements presented in Table 5 in some detail. Consider first the results for HD 19445 for Ca I: the measurements for the line center are presented as corrected to the geocentric radial velocity for frame 1. The difference between frame 4 and frame 1 is −0.22 km s^{-1} due to diurnal motion. The mean and standard deviation of the measured wavelength of Ca I is 6714.882 ± 0.007 Å. The expected uncertainty of an individual measurement of the Ca I can be estimated from Cayrel's (1988) equation (4) using the following parameters: line FWHM ≈ 0.15 Å, pixel size = 0.0265 Å, S/N ≈ 130 (for an individual spectrum), and central line depth = 0.07, which yields an expected error of 0.008 Å. This estimated error for a single measurement is in good agreement with the measured error (0.008 and 0.007 Å, respectively). With four independent measurements, our final uncertainty in the average Ca I wavelengths is thus ±0.004 Å. Adopting a wavelength of 6717.681 Å for the Ca I line (Kurucz Peytremann 1975), the geocentric radial velocity is $v_\oplus = -124.9 \pm 0.2$ km s^{-1}, or a heliocentric velocity of $v_\odot = -139.5$ km s^{-1} for HD 19445 in good agreement with $v_\odot = -140.4 \pm 1.2$ km s^{-1}

TABLE 4

OBSERVED Li LINES AT R = 124,000

Transition	Predicted λ(Å)	Observed λ(Å)	O−P (Å)
Component 1: ^{7}Li 1/2–3/2	6707.761	6707.766	+ 0.005
Component 2: ^{7}Li 1/2–1/2 + ^{6}Li 1/2–3/2	6707.913	6707.917	+ 0.004
Component 3: ^{6}Li 1/2–1/2	6708.072	6708.072	0.000

TABLE 5

WAVELENGTH MEASUREMENTS OF Li I AND Ca I

Star/Frame	S/N	$\lambda_{\rm Li\,I}$	$\lambda_{\rm Ca\,I}$	Δ Ca–Li (Å)	λ_0(Li I)
HD 19445/1	141	6705.007	6714.883	9.876	6707.805
HD 19445/2	112	6705.011	6714.872	9.861	6707.820
HD 19445/3	115	6705.017	6714.890	9.873	6707.808
HD 19445/4	130	6705.020	6714.883	9.863	6707.818
HD 84937/10....	140	6706.888	6716.789	9.901	6707.780
HD 84937/11....	145	6706.898	6716.790	9.892	6707.789
HD 84937/12....	150	6706.905	6716.767	9.862	6707.819
HD 84937/13....	155	6706.921	6716.766	9.845	6707.836
HD 84937/48....	143	6706.896	6716.742	9.846	6707.835
HD 84937/49....	130	6706.907	6716.743	9.836	6707.845
HD 84937/50....	147	6706.904	6716.758	9.854	6707.827
HD 84937/51....	122	6706.915	6716.760	9.845	6707.836

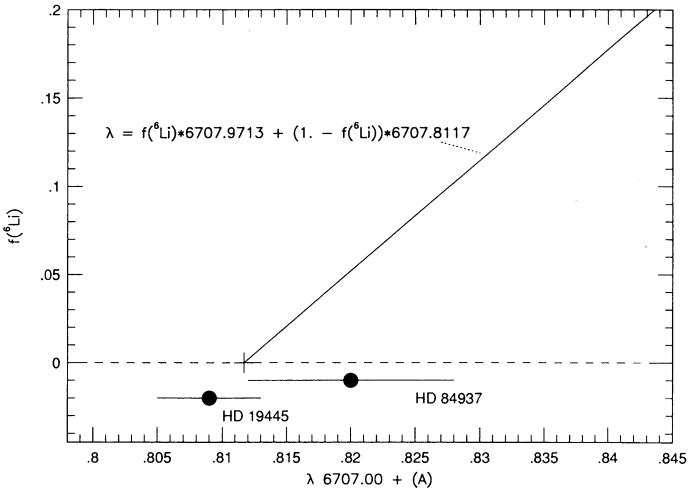

FIG. 4.—Top panel shows how the center-of-gravity (cog) wavelength of the Li I feature shifts toward longer wavelengths with increasing ^{6}Li fraction, $f(^6\mathrm{Li})$: pure ^{7}Li should produce a cog wavelength of 6707.8117 Å, while pure ^{6}Li shifts to 6707.9713 Å. The bottom panel presents the mean, and standard deviation of the mean, cog measurements for the two program stars. The cog wavelength for HD 19445 is consistent with pure ^{7}Li, while HD 84937 has a slightly redshifted cog wavelength, suggesting a possible small contamination by ^{6}Li.

from Carney & Latham (1987). Applying the same corrections to the Li I feature, we measure a mean cog wavelength of 6705.014 ± 0.006 Å: again the standard deviation is near the expected wavelength uncertainty of 0.004 Å based upon the Cayrel formula and the above parameters, except for a central line depth = 0.13. We present also the measured Δ's and resultant λ_0(Li I)'s in Table 5: the mean and uncertainty of this mean is λ_0(Li I) = 6707.813 ± 0.004 Å for HD 19445. One final correction must be applied to this wavelength due to the nonlinear nature of the Doppler shift: at the measured radial velocity of −125 km s^{-1}, the Ca I line is shifted 0.004 Å more to the blue than Li I, thus our λ_0(Li I) must be lowered to λ_0(Li I) = 6707.809 ± 0.004 Å.

The wavelength for the Li I feature can be compared to that expected for an arbitrary mixture of ^{6}Li and ^{7}Li: we adopt the same method as used by Herbig (1964), as well as Andersen et al. (1984). If each component is weighted by its *gf*-value, pure ^{7}Li would produce a cog wavelength of 6707.8117 Å, while pure ^{6}Li would be 6707.9713 Å, and, for weak lines, intermediate mixtures would yield a wavelength between the two isotopes that would be weighted by the respective fractions of ^{6}Li and ^{7}Li,

$$\lambda_0 = f(^6\mathrm{Li})6707.9713 + [1 - f(^6\mathrm{Li})]6707.8117 \text{ Å},$$

where $f(^6\mathrm{Li})$ is the ^{6}Li fraction. In Figure 4 we illustrate such a simple relationship between the cog wavelength and $f(^6\mathrm{Li})$ by the solid line. Note the measured cog for HD 19445: it is in close agreement with $f(^6\mathrm{Li}) \approx 0.00$, and the 2 σ upper limit is $f(^6\mathrm{Li}) \lesssim 0.04$.

The adopted Ca I wavelength comes from energy levels provided by Risberg (1968) from her extensive rediscussion of the Ca I spectrum. Risberg's values are included by Sugar & Corliss (1979) in their critical compilation. For the 6717 Å line, she quotes a measured interferometric wavelength of 6717.685 Å from Wagman (1937). She remarks that the mean absolute difference between the observed wavelengths and the energy levels derived from such wavelengths is 0.016 cm^{-1} or 7 mÅ at 6717 Å. Thus, the 4 mÅ difference is representative of many lines. If the interferometric wavelength were adopted, we would obtain λ_0(Li I) = 6707.813 Å, which is precisely the predicted wavelength for pure ^{7}Li.

The situation for HD 84937 is more interesting. The measured wavelength for Ca I are presented as corrected to the geocentric radial velocity of frame 51: due to the combination of diurnal plus orbital motion over the two nights, there is a difference of −0.46 km s^{-1} between frames 10 amd 51. The mean and standard deviation of the eight Ca I measurements is 6716.764 ± 0.018 Å; the expected wavelength error for this line, using the Cayrel (1986) formula with a central line depth of 0.03, yields $\Delta\lambda \approx 0.018$ Å. The same quantities for the Li I feature are $\bar{\lambda}_{\rm cog}$ = 6706.904 ± 0.010 Å with an estimated error expected to be (central line depth = 0.08) 0.007 Å: again the measured errors and the predicted errors are in good agreement. Given the eight separate measurements, the uncertainties in the average wavelengths of the Ca I and Li I lines are now ±0.006 Å and ±0.004 Å, respectively. With λ(Ca I) = 6716.764 ± 0.006 Å, the geocentric radial velocity is $v_\oplus$ = −40.9 ± 0.3 km s^{-1}, or a heliocentric velocity of $v_\odot$ = −14.2 ± 0.3 km s^{-1} which is in close agreement with $v_\odot$ = −14.9 ± 1.1 km s^{-1} from Carney & Latham (1987). The measured Δ's and λ_0(Li I)'s are presented in Table 5 with the mean and uncertainty of the mean being λ_0(Li I) = 6707.821 ± 0.008 Å for HD 84937. With a measured radial velocity of −40.9 km s^{-1}, the Ca I line is shifted 0.001 Å closer to the Li I line, so the final λ_0(Li I) = 6707.820 ± 0.008 Å. The cog wavelength measured in HD 84937 is 0.011 Å larger than in HD 19445. Note that this difference is independent of the small uncertainty regarding the wavelength of the Ca I line. The difference of the Li I wavelengths is marginally larger than the uncertainties in determining the mean wavelengths and suggests that the intrinsic line profiles in these two stars may be different. This difference in wavelength (see Fig. 4) suggests that either HD 84937 contains a detectable amount of ^{6}Li [$f(^6\mathrm{Li}) \sim 0.05$], or that the stellar wavelengths of Ca I and Li I are shifted in the photosphere with respect to each other: perhaps due to convective motions of order 0.5 km s^{-1} (although such hypothesized motions are *not* in the cooler HD 19445). A more accurate and powerful analysis is provided by an analysis of the Li I line-profiles themselves and we now discuss our results of spectrum synthesis of the stellar lines.

3. SYNTHESIS OF THE Li I PROFILE

3.1. *Model Atmospheres and Stellar Parameters*

The synthesis of the Li I line profile in the spectra of HD 19445 and HD 84937 is based on new flux constant, LTE model atmospheres kindly constructed by B. Edvardsson for the specific atmospheric parameters of the two stars. The models are calculated from the MARCS code of Gustafsson et al. (1975), but include an update to the continuous absorption coefficient, as well as line blanketing from millions of atomic lines with data taken from Kurucz (1989). For a detailed discussion of the models, we refer to Edvardsson et al. (1993).

The effective temperatures were derived from the $(b - y)$ color indices using the recent model atmosphere calibration described by Edvardsson et al. (1992): note that this calibration results in effective temperatures of metal-poor stars that are 50–100 K lower than the $T_{\rm eff}$'s derived from Magain's (1987) empirical $(b - y)$ calibration. The surface gravities were estimated from the position of the stars in the Strömgren c_1–$(b - y)$ diagram for metal-poor stars (see Fig. 1 of Schuster & Nissen 1989). In this "H-R Diagram," HD 84937 is located at the bluest point of the turnoff, whereas HD 19445 is located further down on the main sequence. Using this information and the $T_{\rm eff}$'s of the stars, the surface gravities were derived from the log $T_{\rm eff}$ − log g isochrones of VandenBerg & Bell (1985): an age of 16 Gyr was assumed, but the derived log g-value is not sensitive to this choice.

Metal abundances of the stars were derived from a new set of accurate equivalent widths of weak Fe I lines measured from spectra obtained with the ESO 3.6 m telescope and the CASPEC echelle spectrometer. The analysis of these data are described elsewhere (Nissen et al. 1993); here we emphasize that the [Fe/H] values are based upon new accurate oscillator strengths (Bard, Kock, & Kock 1991; O'Brian et al. 1991) and refer to a solar iron abundance of log ϵ(Fe) = 7.50. The microtubulence parameter, ξ, was determined by requiring that the abundance of a given element be independent of the equivalent width of the line used to derive the abundance. About 30 Fe I lines and 10 Ca I lines, ranging in equivalent width from 5 to 80 mÅ, were used for each star.

Table 6 lists the derived parameters along with the estimated uncertainty of each quantity. Generally, the values of $T_{\rm eff}$, [Fe/H], and ξ agree well with previous determinations, although a slightly higher $T_{\rm eff}$ of HD 84937 is usually quoted. Thus, Magain (1989) determines $T_{\rm eff}$ = 6200 K from the $(b - y)$ and $(V - K)$ color indices. The surface gravities quoted in the literature are often lower than those of Table 6: by forcing Fe I and Fe II lines to yield consistent abundances, Magain (1989) derives gravities of log g = 4.1 for HD 19445 and 3.6 for HD 84937. These lower gravities are, however, in conflict with the position of the stars in the c_1–$(b - y)$ diagram and we suspect that systematic errors in the oscillator strengths used by Magain, and/or non-LTE effects, are present. Taken together, the quoted uncertainties in Table 6 are realistic. In any case, the uncertainties in the model atmosphere parameters turn out to have negligible effects on the ^{6}Li/^{7}Li ratios derived from the synthesis of the Li I line profile.

TABLE 6

PROGRAM STAR MODEL ATMOSPHERE PARAMETERS

Star	$T_{\rm eff}$ (K)	log g	[Fe/H]	ξ (km s^{-1})
HD 19445	5820	4.6	−2.2	1.5
HD 84937	6090	4.0	−2.4	1.5
Error estimate	±100	±0.2	±0.2	± 0.3

3.2. *Determination of the Stellar Broadening*

After the selection of basic stellar parameters ($T_{\rm eff}$, log g, ξ, metallicity) it is critical for the interpretation of the line profile to determine the intrinsic stellar broadening: a combination of microturbulence, macroturbulence, and stellar rotation. Through an analysis combining both strong and weak lines from the same species, the microturbulence is found as discussed in § 3.1. The Ca I 6162.172 Å line in both HD 19445 and HD 84937 is used to determine the underlying macroturbulence plus v sin i. The first step is to use the integrated equivalent width of the Ca I line, along with the given microturbulences, to derive the Ca abundance: the Ca I equivalent widths are 42.5 and 58.8 mÅ for HD 19445 and HD 84937, respectively. Once the Ca abundance is established, the Ca I 6162 Å region can be synthesized and the broadening required to provide the best fit to the line profile can be measured. This broadening parameter is assumed to consist of a convolution of the instrumental profile of the spectrometer and the underlying stellar profile: the synthesis program includes the thermal plus microturbulent motions in the output "raw" synthetic spectrum. This raw synthetic spectrum is always found to be narrower than the stellar spectrum and is broadened by a Gaussian function of specified width to better fit the observed profile. In rapidly rotating stars, the line profile assumes a parabolic shape, but we find that both HD 19445 and HD 84937 are quite slow rotaters and we are unable to determine whether the underlying stellar broadening is dominated by Gaussian-like macroturbulence or stellar rotation. We will thus characterize the stellar broadening by a single parameter: the half-width of the Gaussian broadening function (which can be expressed as either a velocity or a wavelength). This broadening parameter is just a convolution of the instrumental profile plus the stellar broadening (the synthesis includes thermal plus microturbulent motions). We determine the instrumental profile from fitting the Th emission comparison lines (again, fitting them with Gaussian forms) and then measure the stellar broadening by assuming that the total broadening parameter consists of the Gaussian quadrature sum of instrumental and stellar:

$$\text{Total}^2 = \text{Instrumental}^2 + \text{Stellar}^2 .$$

The broading parameters were determined by comparisons of the observed spectra to synthetic spectra; the best fit between observed and synthetic spectra was taken to be that which gave the minimum differences in the summation of (observed − synthesis) versus wavelength, here $\sum$ (O − S). In such a diagram, a "perfect" fit would manifest itself as noise scattering about zero: small mismatches in the slope of the continuum between real star and synthesis would yield a slowly varying, but steady, increase or decrease in the sum of (observed − synthesis). A failure to fit a line profile would result in a sharp, almost discontinuous change in the $\sum$ (O − S). We choose this form to fit the synthesis to the observations because these discontinuous changes are easy to detect and measure.

In Figure 5 we show the Ca I line in HD 19445 (*filled circles*) and the best-fit synthesis (*solid line*): the synthesis is defined by the Ca abundance [log ϵ(Ca) = 4.38] and microturbulence (1.5 km s^{-1}). The line list used for this synthesis utilized a solar

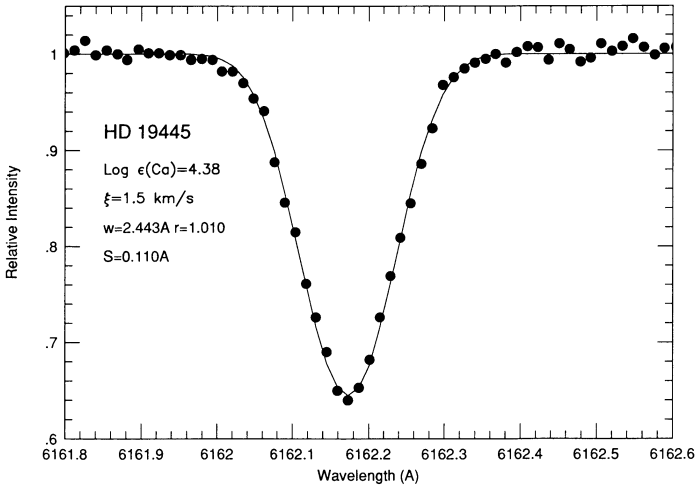

FIG. 5.—Comparison of the observed and synthetic spectra near the Ca I 6162.17 Å line in HD 19445: the filled circles are the observed points and the solid curve the best synthetic match. The Ca abundance is set by the integrated equivalent-width plus microturbulence, while the observed stellar radial-velocity sets the wavelength shift (w), and the continuum points on either side of the line set the continua match (r). The best smoothing which then fits the line is shown: $S = 0.110$ Å.

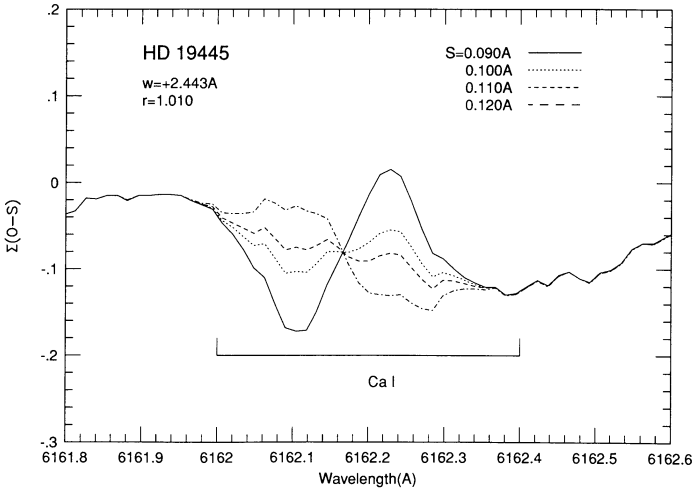

FIG. 6.—Sum of (observed − synthesis), $\sum$ (O − S), across the Ca I 6162.17 Å line for HD 19445 for various smoothing parameters, S. The approximate extent of the Ca I line is shown by the bracket. Very low-amplitude, long-wavelength mismatches in the continua are present (residual fringing), however, these have no effect on fitting the line-profile, and the large, sharp, almost discontinuous signals in $\sum$ (O − S) are evident for the wrong smoothing. The best fit is provided by $S = 0.110$ Å, which, given the intrinsic spectrometer broadening of 0.0464 Å, implies an underlying stellar broadening of 0.100 Å, or about 4.9 km s^{-1}, in velocity space.

gf-value (derived using a Holweger & Müller 1974 solar atmosphere) for the Ca I, with additional lines from the Kurucz & Peytremann (1975) compilation. Fitting the synthesis to the real spectrum requires a radial velocity shift (here $w = +2.443$ Å), a slight shift to the empirical stellar continuum to fit the synthesis (here $r = 1.010$), and, finally, the smoothing factor (which we label S). Both w and r are very well defined (differences in w of 0.005 Å or 0.003 in r significantly degrade the fits) with high S/N spectra and a well-defined continuum: both of these criteria are satisfied for our metal-poor program stars. By varying the smoothing by quite small amounts, significant changes in the fit to the line profile occur: we illustrate this in Figure 6, where we show the summation of the (observed-synthesis) points (this can be thought of as the integral of the differences between two curves) as a function of wavelength (we expand the region just around the Ca I line) for different smoothing parameters. As can be seen, there are slow variations in the fit to the continuum (this is analogous to low-frequency noise) due to some residual nonflatness in the continuum-flattened observed spectrum, however, these variations exist on much larger scales than spanned by a spectral-line profile. The mismatches to the Ca I profile are clearly evident for the different smoothings for HD 19445 in Figure 6. The optimum value of S is that which provides a smooth connection of the continuum across the line profile: for HD 19445, this smoothing is $S = 0.110$ Å, with an uncertainty of about 0.005 Å.

From measurements of Th lines observed with this same spectrometer setup, we determine that the Gaussian FWHM is 0.0464 Å, so the underlying stellar broadening in HD 19445 can be characterized by a Gaussian of FWHM^2 = $(0.110)^2 - (0.0464)^2$, or FWHM = 0.100 Å or 4.9 km s^{-1}. This broadening consists mainly of macroturbulence plus rotation ($v \sin i$): this is consistent with what is observed for dwarf stars near this $T_{\rm eff}$.

In Figure 7 we show the observed Ca I line in HD 84937 and the best synthetic fit for the parameters listed on the figure. Figure 8 then illustrates the $\sum$ (O − S) diagram for the Ca I line for various smoothing factors, S. For HD 84937, we find that $S = 0.140$ Å provides the best fit between observation and synthesis and gives a smooth curve through the line profile with a minimum of discontinuous steps. This spectrum was obtained with the same spectrometer setting as HD 19445, so this broadening implies an underlying stellar broadening defined by a Gaussian FWHM = 0.132 Å or 6.4 km s^{-1}.

The adopted smoothing factors have been applied to the weak Ca I 6717 Å line. The fits to both the HD 19445 and HD 84937 profiles are within the expected uncertainties set by the S/N ratios. Since one set of smoothing factors fits Ca I lines weaker (6717 Å) and stronger (6162 Å) than the Li I line of a given star, we have confidence that they represent the correct smoothing factors for the latter line.

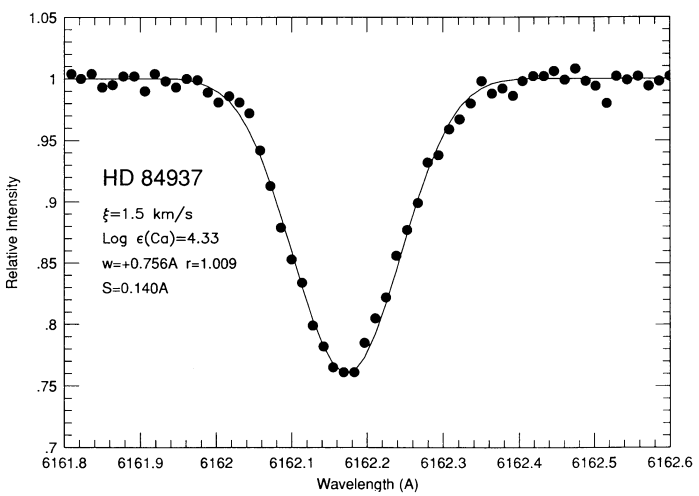

FIG. 7.—Ca I 6162.17 Å region in HD 84937: the filled circles are the observed points, and the solid curve is the best-fit synthesis. The Ca abundance is indicated, as well as the wavelength shift (w), the continuum adjustment (r), and the best-fit smoothing of $S = 0.140$ Å.

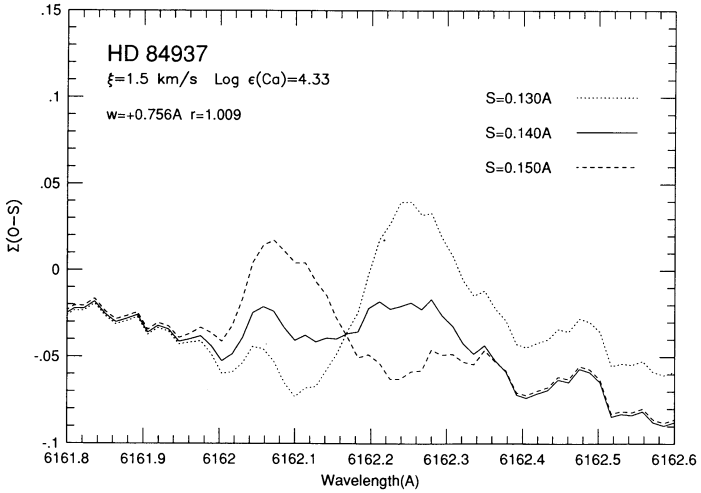

FIG. 8.—Close-up of $\sum$ (O − S) across the Ca I 6162.17 Å line in HD 84937 for various values of the smoothing parameter, S. Smoothings of 0.130 and 0.150 Å yield large residual signals in $\sum$ (O − S), while $S = 0.140$ Å provides the smoothest fit across the Ca I line profile.

Detection of ^{6}Li in HD 84937 is based on a slight increase of the Li I line's inherent asymmetry. In principle, stellar granulation may mimic the asymmetry attributed to ^{6}Li. We discount this possibility on the grounds that the Ca I line profiles are highly symmetric. The maximum allowable asymmetry is too small to have induced the additional asymmetry that we attribute to ^{6}Li in HD 84937.

3.3. *Estimate of the* ^{6}Li *Content*

Given that we have characterized the intrinsic stellar broadening in the two program stars, we can now apply spectrum synthesis to the Li I line profile. We begin by setting the abundance of total Li from the integrated equivalent-width of the Li I line: we derive the Li abundance using the model atmospheres and the microturbulence given in Table 6, as with the 6162 Å Ca I line. The equivalent widths of the Li I 6707 Å lines are listed in Table 1, where the average of the measurements are W_λ(Li I) = 35.4 ± 1.2 mÅ and W_λ(Ca I) = 10.8 ± 1.0 mÅ for HD 19445 and W_λ(Li I) = 25.3 ± 1.2 mÅ and W_λ(Ca I) = 6.5 ± 0.7 mÅ for HD 84937. In fitting the line profiles, we use the averaged spectra (illustrated in Figs. 1 and 2) and the equivalent widths from the averaged spectra are W_λ(Li I) = 35.4 mÅ and W_λ(Ca I) = 10.3 mÅ for HD 19445 and W_λ(Li I) = 25.1 mÅ and W_λ(Ca I) = 6.5 mÅ for HD 84937: these agree very well with the average of the measurements from the individual spectra.

We begin with an illustration of the fit to the Li I line profile in HD 19445 in Figure 9: here the filled circles are the observations and the continuous curves are two syntheses. With the combination of $T_{\rm eff}$/log g/[M/H]/ξ and the total integrated equivalent width, the total Li abundance is set. The intrinsic stellar broadening is determined from the Ca I 6162 Å line, so the smoothing is set: the intrinsic stellar broadening was found to be 4.9 km s^{-1}, or 0.110 Å at 6707.8 Å, while the Th lines yield a FWHM = 0.0538 Å and the broadening applied to the synthetic spectra is $[(0.110)^2 + (0.0538)^2]^{1/2}$ Å = 0.122 Å. This Gaussian broadening has been applied to the synthetic spectra in Figure 9 where two ^{6}Li fractions are shown: $f(^6\text{Li}) = 0.00$ and 0.10. The wavelength shift applied to the observed spectrum to bring the observed and synthetic spectra into agreement is $w = +2.792$ Å, or an apparent radial velocity of $v_\oplus = -124.8$ km s^{-1}, or $v_\odot = -139.4$ km s^{-1}, and is in excellent agreement with the result from the Ca I 6162 Å line ($v_\odot = -139.8$ km s^{-1}) observed on a different date (see Fig. 5). A small shift between the observed and synthetic continua (observed is multiplied by $r = 1.005$) is required to minimize the differences between (observed − synthesis) from ~1 Å bands on either side of the Li I feature and the comparison is shown in Figure 9. Clearly, $f(^6\text{Li}) = 0.00$, i.e., no ^{6}Li at all, provides an excellent fit to the Li I line profile, while increasing the ^{6}Li fraction to 10% misses completely the observed core and red wing of the line. The difference between the observed and synthetic spectra, in the form of $\sum$ (O − S), is illustrated in Figure 10 for the region around 6707–6708 Å. We show three syntheses with $f(^6\text{Li}) = 0.00$, 0.03, and 0.05: a value of $f(^6\text{Li}) = 0.10$ is an even worse fit and we do not show it here in Figure 10. The positions and relative gf-values of the main Li I components are shown: for $f(^6\text{Li}) = 0.05$ and 0.03, discontinuities across the Li profile are evident, while $f(^6\text{Li}) = 0.00$ yields a smooth difference of $\sum$ (O − S) through the entire Li I profile. At the noise level of the continuum fit between $\sum$ (O − S) we can reject even $f(^6\text{Li}) = 0.02$: for HD 19445 then, $f(^6\text{Li}) = 0.00$, with a strong upper limit of, at most, 2% ^{6}Li. Recall the cog λ_0(Li I) for HD 19445 (Fig. 4) where we also find a result consistent with $f(^6\text{Li}) = 0.00$. Using both techniques, wavelength determination and profile fitting, we find HD 19445 to be a halo dwarf with the plateau Li abundance [log ϵ(Li) = 2.12] and $f(^6\text{Li}) = 0.00$.

In Figure 11 is shown the comparison and synthetic spectra for HD 84937: as in Figure 9, the filled circles are the observations and the continuous curves show three syntheses. The total Li abundance, derived from the integrated equivalent width of Li I, is log ϵ(Li) = 2.12 and the intrinsic stellar broadening, determined from the Ca I 6162 Å lines, has been taken to be 6.4 km s^{-1}, or 0.143 Å at 6707.8 Å. The Th lines yielded an instrumental FWHM = 0.0538 Å and the broadening applied to the synthetic spectra is thus $S = [(0.143)^2 + (0.0538)^2]^{1.2} = 0.153$ Å. As with HD 19445, the

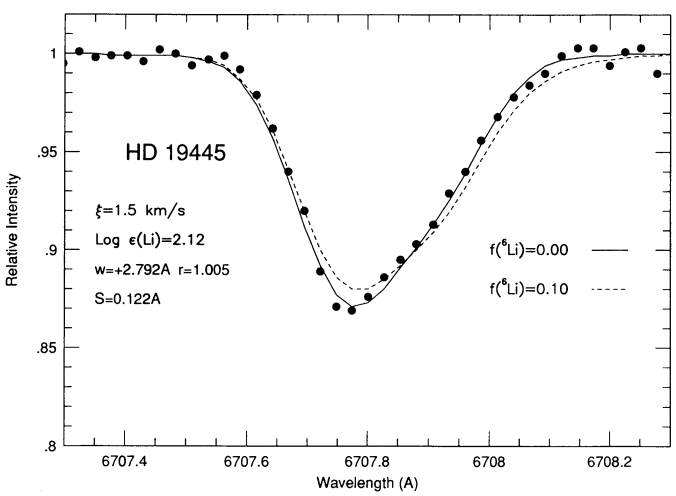

FIG. 9.—Li I line profile in HD 19445: the filled circles are the observed points, and the continuous curves are the synthetic spectra for two values of $f(^6\text{Li})$. The Li abundance is set by the integrated equivalent width, while the wavelength shift is defined by the blue line-wing and the continua are matched on either side of the line and set by r. The smoothing has been defined by the Ca I 6162.17 Å. It is clear, even to the eye, that $f(^6\text{Li}) = 0.00$ is quite a good fit to HD 19445, while 10% ^{6}Li misses badly both the core and the red wing of the Li I profile.

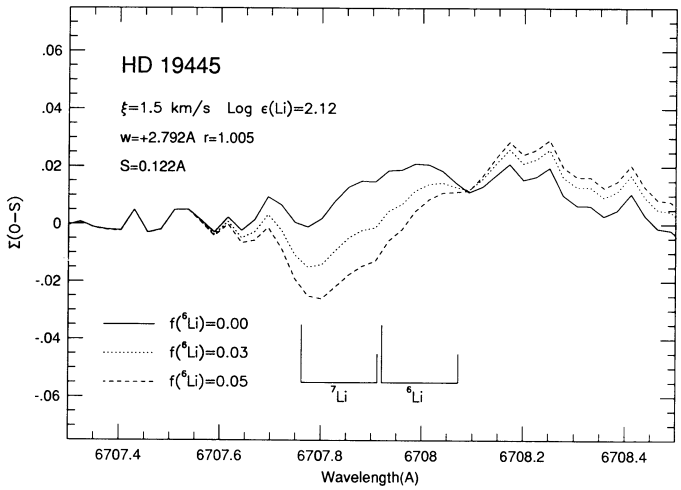

FIG. 10.—Sum of the (observed − synthesis) residuals across the Li I line in HD 19445: results for three mixtures of $f(^6\mathrm{Li}) = 0.00$, 0.03, and 0.05 are shown [clearly from Fig. 10, $f(^6\mathrm{Li}) = 0.10$ was a poor fit]. The positions and relative strengths of the Li components are shown, and 5% ^{6}Li produces a negative residual signal through the line core, followed by a positive signal across the red line-wing. This same mismatch is seen for $f(^6\mathrm{Li}) = 0.03$, but with a smaller amplitude, while no ^{6}Li provides a smooth, almost zero residual signal, across the Li I line profile.

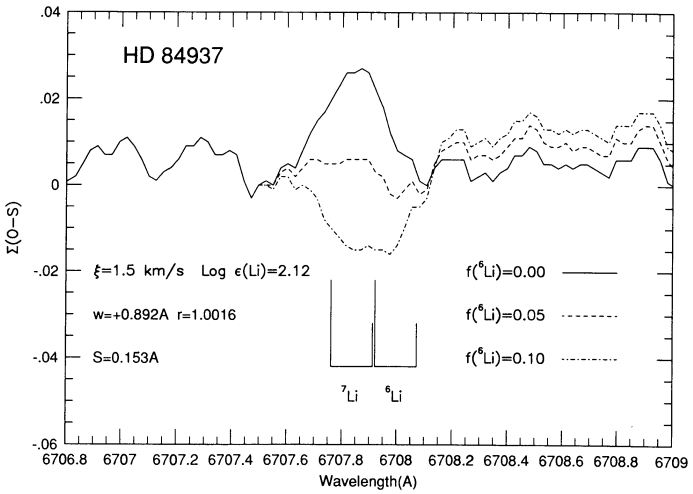

FIG. 12.—$\sum$ (O − S) residuals across the Li I line in HD 84937: the mixtures with $f(^6\mathrm{Li}) = 0.00$ and 0.10 produce strong residuals through the Li I line, but 5% ^{6}Li yields a smooth fit through the entire line profile.

comparison of observed to synthetic continuum level has been set by using the regions that are 1 Å on either side of the Li I feature and required that the observed continuum in this region be raised by 0.16% ($r = 1.0016$). The observed wavelength shift of $w = +0.892$ Å, or an apparent radial velocity of $v_\oplus = -39.9$ km s^{-1}, leads to $v_\odot = -13.3$ km s^{-1}, in good agreement with $v_\odot = -14.2$ km s^{-1} as determined by the Ca I 6162 Å line observed on a different date (see Fig. 7). From Figure 11, it is apparent that the synthesis with $f(^6\mathrm{Li}) = 0.00$ misses the core and red edge of the Li I feature, while $f(^6\mathrm{Li}) = 0.10$ has too much ^{6}Li, but $f(^6\mathrm{Li}) = 0.05$ provides a good fit to the entire line profile. The fit of $f(^6\mathrm{Li}) = 0.05$ is even more evident in Figure 12, where we again present $\sum$ (O − S) versus wavelength: the discontinuities in the comparison of observed to synthetic at the wavelength of the Li feature are clear for $f(^6\mathrm{Li}) = 0.00$ and 0.10: $f(^6\mathrm{Li}) \approx 0.05$, on the other hand, provides a smooth comparison through the entire Li I profile. Changing $f(^6\mathrm{Li})$ by ± 0.02 degrades the smooth comparison and a detectable discontinuity appears across the wavelength of the ^{6}Li feature. Based upon the best determination of stellar broadening, the Li I feature in HD 84937 requires a detectable amount of ^{6}Li of about 5% of total Li. Analyzing each night's spectra separately leads to the same result as found for the combination of both night's data. Referring back to Figure 4, we note that the cog of λ_0(Li I) in HD 84937 also indicates a small, but measurable, amount of ^{6}Li, but with large uncertainties: thus, both the wavelength determination and line-profile synthesis in HD 84937 suggest a measurable amount of ^{6}Li in the atmosphere. We find that HD 84937, a hotter halo dwarf than HD 19445, also contains the plateau Li abundance [log ϵ(Li) = 2.12] but $f(^6\mathrm{Li}) = 0.05$; this result is in agreement with the upper limit of $f(^6\mathrm{Li}) \lesssim 0.10$ by Pilachowski, Hobbs, & de Young (1989) for HD 84937.

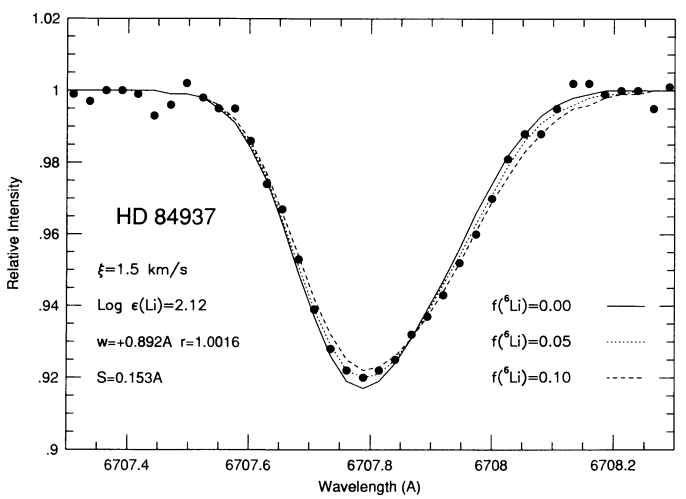

FIG. 11.—Li I line-profile in HD 84937: the filled circles are the observed points, and three synthetic spectra, with $f(^6\mathrm{Li}) = 0.00$, 0.05, and 0.10, are shown. With the values of w, r, and S (as derived from the Ca I 6162.17 Å line), it is apparent that the synthesis with no ^{6}Li misses the core and red wing of the Li I line-profile. A value of $f(^6\mathrm{Li}) = 0.10$ misses in the opposite sense from $f(^6\mathrm{Li}) = 0.00$, whereas $f(^6\mathrm{Li}) = 0.05$ yields an apparently smooth fit.

We now discuss the uncertainties of the line-profile analysis and ascertain whether HD 84937 can be fit with no ^{6}Li.

3.4. *Uncertainties*

We investigate the uncertainties in the estimate of the ^{6}Li content by varying those parameters necessary to fit the Li I profile. The parameters needed to interpret the line profiles can be thought of crudely as being of two types: the model atmosphere variables, $T_{\rm eff}$/log g/ξ, which affect the total abundance from the integrated equivalent-width (and through the abundance, the line profile), and the variables derived more directly from the observed spectrum itself, namely the wavelength shift (w), the continuum adjustment (r), and the smoothing (S). Of course, the underlying smoothing, S, must depend upon the abundance to some degree, however, as we shall show, the changes in S with plausible changes in $T_{\rm eff}$, log g, or ξ are very small, and S could quite satisfactorily be measured without regard to a model-atmosphere synthesis, but directly from the spectrum. Due to the fact that we detect ^{6}Li in HD 84937, we concentrate on this star and estimate how much $f(^6\mathrm{Li})$ can be changed by changing atmospheric and spectroscopic parameters.

First, we change the model atmosphere's $T_{\rm eff}$ and estimate what change this would bring about in the derived $f(^6\mathrm{Li})$. A model about 50 K hotter was tried at $T_{\rm eff} = 6135$ K; beginning with Ca I 6162 Å, this increases the Ca abundance to $\log \epsilon(\mathrm{Ca}) = 4.36$ from 4.33. Determining the smoothing via $\sum (\mathrm{O} - \mathrm{S})$, as in Figure 8 for $T_{\rm eff} = 6090$ K, yields $S = 0.143$ Å as compared to $S = 0.140$ Å at $T_{\rm eff} = 6090$ K: this smoothing implies a slight increase in the stellar broadening from 6.4 km s^{-1} to 6.6 km s^{-1} and requires a broadening at Li I 6707 Å of 0.157 Å $= [(0.148)^2 + (0.0464)^2]^{1/2}$ Å. This is an increase of 0.004 Å in S and we illustrate these syntheses in Figure 13: this figure is very similar to Figure 11 and indicates little sensitivity in $f(^6\mathrm{Li})$ if $T_{\rm eff}$ is changed by as much as 100 K. This same result holds for changes in $\log g$ and we must conclude that uncertainties in $T_{\rm eff}$ and $\log g$ contribute very little to uncertainties in the derived $f(^6\mathrm{Li})$.

As the underlying stellar broadening is assumed to be rotation plus macroturbulence, we investigate changing the microturbulence between 1.0 and 2.0 km s^{-1}. Changing ξ from 1.5 km s^{-1} to 1.0 km s^{-1} increases $\log \epsilon(\mathrm{Ca})$ to 4.41, from 4.33, using the Ca I 6162 Å line, and we find a slight increase in S of +0.002 Å. The Li abundance, being derived from a rather weak line, remains the same [$\log \epsilon(\mathrm{Li}) = 2.12$] at $\xi = 1.0$ km s^{-1} and the tiny increase in S found by lowering ξ does not lower measureably $f(^6\mathrm{Li})$. Likewise, increasing ξ to 2.0 km s^{-1} lowers $\log \epsilon(\mathrm{Ca})$ to 4.27 and leads to a slightly smaller value of S by about the same amount (~ -0.002 Å) but does not measureably change $f(^6\mathrm{Li})$. Likely combinations of $T_{\rm eff}$, $\log g$, and ξ will not lead to substantial (or even measureable) changes in $f(^6\mathrm{Li})$.

The quantity which most affects $f(^6\mathrm{Li})$ is S. To a lesser degree, the continuum level, r, and the radial-velocity wavelength shift, w, influence a fit between observed and synthetic spectra; however, r is strongly constrained by the fact that both program stars are very metal-poor (i.e., no other detectable lines) and the S/N ratios are quite high while w can be changed by only a small amount ($\sim$0.005 Å at 6707 Å), otherwise the observed and synthetic line profiles become completely mismatched. An experiment in smoothing is shown in Figure 14: here we have taken the Li abundance set by the equivalent width [$\log \epsilon(\mathrm{Li}) = 2.12$] and artificially increased the smoothing and adjusted the wavelength shift to fit the profile with $f(^6\mathrm{Li}) = 0.00$. A good fit can be accomplished with no ^{6}Li if $S = 0.170$ Å (an increase of 0.17 Å over the fit using the Ca I 6162 Å line) and w is decreased slightly by 0.005 Å (from 0.892 to 0.887 Å). The increased smoothing implies an underlying stellar broadening of 7.2 km s^{-1} (compared to 6.4 km s^{-1} from our "best estimate" fit) and a heliocentric radial velocity of -13.0 km s^{-1} compared to -13.3 km s^{-1}, as derived from w. We can now apply this increased broadening to the Ca I 6162 Å line ($S = [(0.148)^2 + (0.0464)^2]^{1/2} = 0.155$ Å) and these results are shown in Figure 15. As can be seen by inspection of the upper panel, the synthetic spectrum is a poor fit to the

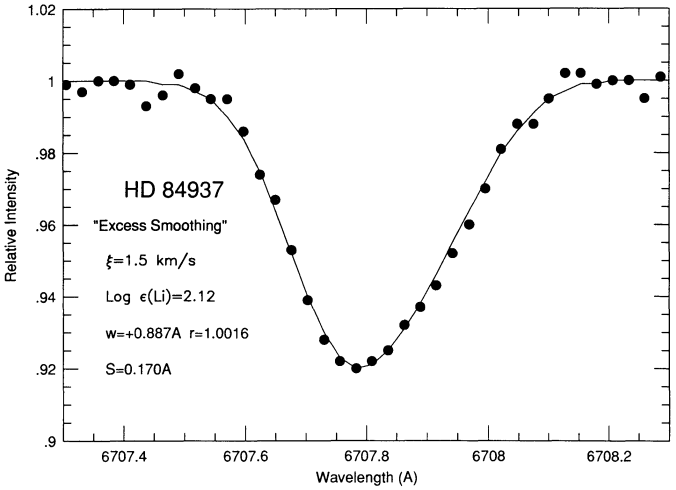

FIG. 14.—Attempt to fit the observed Li I line in HD 84937 (*filled circles*) with $f(^6\mathrm{Li}) = 0.00$ by artificially increasing the smoothing, S, and adjusting w. A tolerable fit can be obtained by increasing S to 0.170 Å (from 0.153 Å) and lowering w by 0.005 Å: it is found, however, that this larger smoothing gives an unacceptable fit to the Ca I 6162.17 Å line.

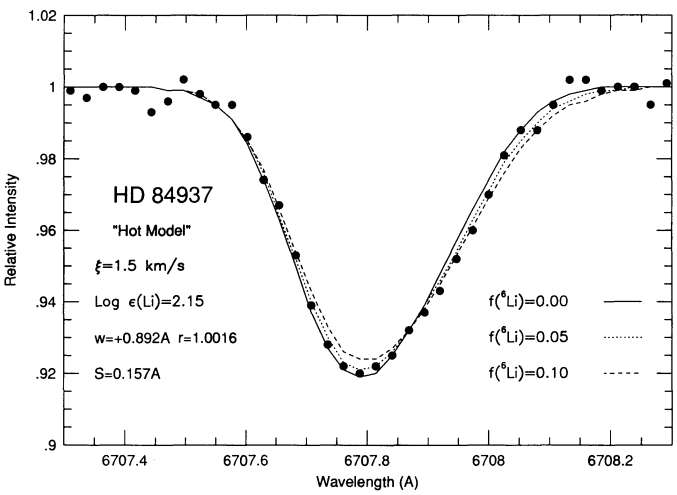

FIG. 13.—Li I line-profile HD 84937 (filled circles are the observed points) with three synthetic spectra (*continuous curves*) generated from a hotter ($T_{\rm eff} =$ 6135 K) model atmosphere. Compared to the best model atmosphere, the Li abundance is increased by +0.03 dex and the smoothing (derived from the Ca I 6162.17 Å line) is increased by +0.004 Å, however, the best estimate for $f(^6\mathrm{Li})$ is not changed significantly using this hotter model atmosphere.

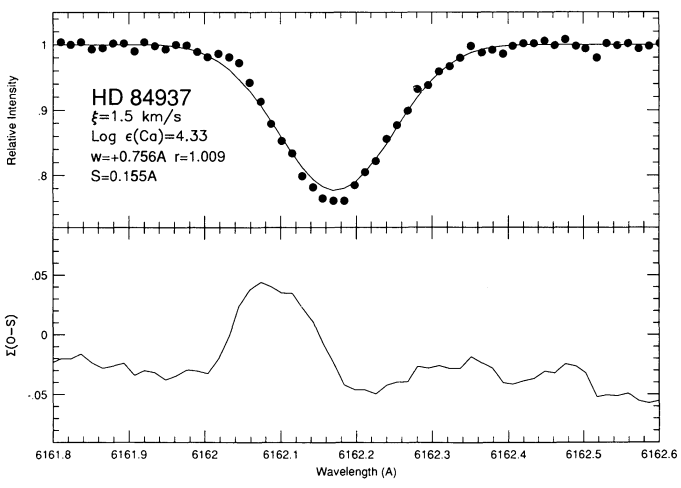

FIG. 15.—Illustration of the fit to the Ca I line using the artificially large smoothing necessary to fit the Li I line in HD 84937 with no ^{6}Li: S has increased here to 0.155 Å, compared to the best fit to the Ca I line of 0.140 Å. The top panel shows the line profiles (filled circles are the observed points, and the continuous curve is the synthesis) while the bottom panel shows the sum of the residuals. The wings and core are not fit and this smoothing is too large: changing the Ca abundance will not improve the fit.

observed spectrum; this is even clearer in the bottom panel of Figure 15 where $\sum$ (O − S) is plotted. A clear, strong difference is shown here with a large discontinuity in $\sum$ (O − S) across the line core, and a comparison with $S = 0.140$ Å in Figure 8 demonstrates that $S = 0.155$ Å is an unacceptable fit. Various combinations of $T_{\rm eff}$/log g/ξ and $r/w/S$ are unlikely to yield $f(^6\mathrm{Li}) = 0.00$ for HD 84937, and we are forced to conclude that $f(^6\mathrm{Li}) = 0.05 \pm 0.02$ for this star, with the additional result that $f(^6\mathrm{Li}) \approx 0.00 \pm 0.02$ for HD 19445.

If varying our simple parameters is unable to remove ^{6}Li from HD 84937, we now ask what complication might be added to "mimic" a ^{6}Li detection? Clearly, both the cog wavelength analysis and the profile analysis point to a redshifted asymmetry in the Li I feature in HD 84937 when compared to HD 19445. This feature can be isolated, for visual purposes, by subtracting the synthetic spectrum, using the "best" parameters for HD 84937 with $f(^6\mathrm{Li}) = 0.00$, from the observed spectrum for HD 84937: this is illustrated by the filled circles in Figure 16. These residuals have been smoothed by a three-point running mean to increase the S/N. The position of the ^{6}Li doublet is indicated and the coincidence in wavelength, with the 4.5 σ absorption feature in the residuals, is perfect. There is no spectral line from some other element, whose abundance might be inexplicably enhanced, that can explain this feature, so the only possibility might be redshifted ^{7}Li itself at $v \sim +8$ km s^{-1}: this scenario seems unlikely due to the large velocity required relative to photospheric ^{7}Li. In addition, we show a synthesis for HD 84937 with no ^{7}Li, but ^{6}Li at log $\epsilon(^6\mathrm{Li}) = 0.82$ [$f(^6\mathrm{Li}) = 0.05$ for log ϵ(Li) = 2.12], in Figure 16 (*solid line*). The ^{6}Li synthesis is a fair reproduction of the observed residuals.

Our analysis has assumed that both stars are single, however, we point out that both HD 19445 and HD 84937 are flagged as possible spectroscopic binaries by Carney & Latham (1987) due to the fact that the scatter in radial velocity measurements for these two stars are larger than expected: $v_\odot = -140.4 \pm 2.1$ km s^{-1} for HD 19445 and $v_\odot = -14.9 \pm 1.1$ km s^{-1} for HD 84937. We note that the average of our Ca I 6717 Å and Li I 6707 Å velocities (obtained from the same spectra) plus Ca I 6162 Å measured about 2 weeks later, are $v_\odot = -139.6 \pm 0.2$ km s^{-1} for HD 19445 and $v_\odot = -13.9 \pm 0.5$ km s^{-1} for HD 84937. Our velocities agree well with the averages from Carney & Latham (1987), thus we cannot, at this time, shed any more light on the question of whether the program stars might be binaries. There is no hint of a secondary spectrum in our Ca I 6162 Å spectra and the feature responsible for the asymmetry in the Li I line-profile in HD 84937, as isolated in Figure 16, is shifted by over +7 km s^{-1} from the main component: such a velocity shift is incompatible with the observed scatter in the radial velocities, unless a hypothesized orbit was very eccentric and we observed the star very near periastron passage. In the future, however, we encourage continued radial-velocity monitoring of these two stars.

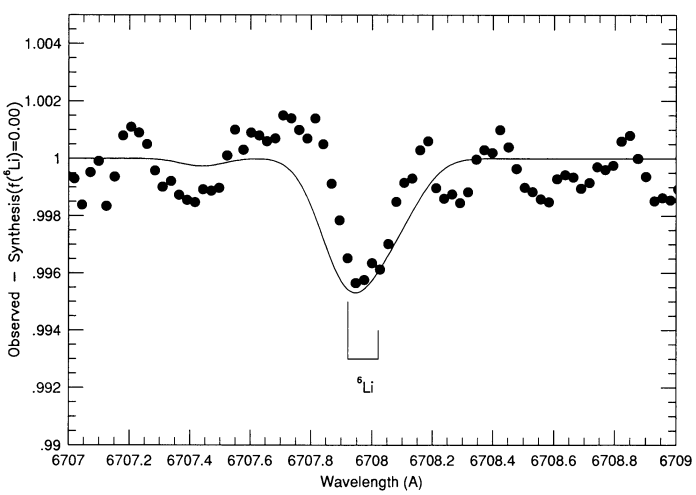

FIG. 16.—Attempt to isolate and illustrate the possible ^{6}Li feature in HD 84937; we plot the residuals (*filled circles*) of (observed − synthesis + 1) with no ^{6}Li in the synthesis: the residuals are noisy and have been smoothed with a three-point running mean. A perfect comparison would yield noise centered on 1, however, a missing absorption feature in the synthesis would show as an apparent absorption feature in the residuals: such a feature is present at exactly the wavelength of the ^{6}Li doublet, as shown. The solid curve is a synthesis with the ^{7}Li removed and log $\epsilon(^6\mathrm{Li}) = 0.82$ [the value if log ϵ(Li) = 2.12 and $f(^6\mathrm{Li}) = 0.05$]. Although the comparison is not perfect, it is apparent that the line profile in HD 84937 can be explained as a combination of about 95% ^{7}Li and 5% ^{6}Li.

4. DISCUSSION

4.1. *Production of* Li *by Cosmic Rays*

Lithium nuclei now observed in halo stars were synthesized in the big bang (and, perhaps in other speculative pre-Galactic sites) and by cosmic rays in the early Galaxy (and possibly also before the formation of the Galaxy). After the formation of the halo stars, lithium may have been depleted in the observable atmospheres. In recognition of the likely principal sources of Li and the different depletion factors for ^{6}Li and ^{7}Li, we write the present Li (= ^{6}Li + ^{7}Li) abundance as

$$\mathrm{Li} = D_7\,{}^7\mathrm{Li}_{\rm BB} + D_6\,{}^6\mathrm{Li}_{\rm BB} + D_7\,{}^7\mathrm{Li}_{\rm CR} + D_6\,{}^6\mathrm{Li}_{\rm CR} \qquad (1)$$

and the present isotopic ratio $R = {}^6\mathrm{Li}/\mathrm{Li}$

$$R = \frac{D_6({}^6\mathrm{Li}_{\rm BB} + {}^6\mathrm{Li}_{\rm CR})}{\mathrm{Li}}\,. \qquad (2)$$

The subscripts BB and CR denote the two different origins of ^{6}Li and ^{7}Li, and the depletion factors are given as D_7 and D_6. In this section, elemental symbols denote abundances with respect to H on the scale $H = 10^{12}$. Since B and Be are synthesized by cosmic rays and most probably not by the big bang, we may use the B and Be abundance to assess the production of Li by cosmic rays. We introduce two quantities that we later estimate from the B abundance and a model of nucleosynthesis by cosmic rays: P and r where ${}^6\mathrm{Li}_{\rm CR} = P\,\mathrm{B}_{\rm CR}$ and ${}^7\mathrm{Li}_{\rm CR} = r\,{}^6\mathrm{Li}_{\rm CR}$. Then, ${}^6\mathrm{Li}_{\rm BB}$ may be rewritten as

$${}^6\mathrm{Li}_{\rm BB} = \frac{R\,\mathrm{Li}}{D_6} - P\,\mathrm{B}_{\rm CR}\,. \qquad (3)$$

In the following discussion, we use the observed/inferred B abundance to predict ${}^6\mathrm{Li}_{\rm CR}$ and ${}^7\mathrm{Li}_{\rm CR}$, i.e., r and P. Then we use the predicted depletion factor D_6 to infer the contribution ${}^6\mathrm{Li}_{\rm BB}$ that is needed to account for the observed small fraction of ^{6}Li in HD 84937. Depletion of ^{6}Li in HD 19445, a cooler and less massive star than HD 84937, is predicted to be so complete that ^{6}Li is not expected to survive. This prediction is consistent with our failure to detect ^{6}Li in HD 19445. In the discussion, we also pay attention to the fact that the Li abundances of the warm halo stars define a "plateau" such that the Li abundance is independent of metallicity: Deliyannis,

Pinsonneault, & Duncan (1993) show that differences in the observed Li abundances over the range [Fe/H] = −1.4 to −3.5 are very small, certainly less than 10%. This observational constraint limits the contributions of the cosmic rays relative to the big bang contribution to the Li abundance. Another possible constraint arises because the Li plateau is defined by stars of differing masses and, hence, with differing surviving fractions of their initial ^{6}Li abundances. In practice, a full exploitation of the latter two constraints must await data on the isotopic ratio in a larger sample of stars.

Identification of B and Be as products of spallation reactions is based on the fact that the observed abundance ratio of B/Be ≅ 10 is that predicted for synthesis by spallation reactions between high-energy cosmic rays and ambient heavy nuclei; i.e., primarily interactions between protons and oxygen nuclei—see Duncan, Lambert, & Lemke (1992), Gilmore et al. (1992), and Prantzos, Cassé, & Vangioni-Flam (1993). The fact that the Be and B abundances are proportional to the stellar O abundances suggests that B and Be had a negligible abundance at the onset of stellar nucleosynthesis (i.e., at zero O abundance) and, hence, the big bang and protogalactic contributions to the Be and B abundances are very small relative to the observed abundances in stars like HD 84937 and HD 19445. In principle, the linear dependence of Be and B on O is consistent with an identification of the light elements as the fruits of stellar nucleosynthesis. However, neutrino-induced spallation, which has been proposed for ^{11}B and Be production in supernovae is expected to give a much higher than observed B/Be ratio: Malaney (1992) estimates B/Be ≅ 200. (Of course, the location of the spallation reactions could be transferred to stellar flares on the surfaces of the stars.) By contrast with the neutrino induced spallation, B/Be ≅ 10 is a firm prediction for high-energy cosmic rays. Note that Prantzos et al. argue that the cosmic rays in the halo should have been dominated by the high-energy particles. Unfortunately, although we may know that Be and B are synthesized by cosmic rays, a prediction of the associated production of ^{6}Li and ^{7}Li (i.e., the factors r and especially P) is beset with additional uncertainties.

In the standard model (Steigman & Walker 1992), Be and B are synthesized by spallation of interstellar CNO nuclei by cosmic-ray protons and alphas with the principal contribution expected to come from the proton-oxygen collisions. Then, we may write the production rate as

$$d\mathrm{B}/dt = \langle \phi_p \sigma_{p\mathrm{O}}(\mathrm{B}) \rangle n_{\mathrm{O}} ,$$

where ϕ_p is the cosmic-ray proton flux, $\sigma_{p\mathrm{O}}(\mathrm{B})$ is the spallation cross section for B production from p-O collisions, angle brackets denote an integral over the cosmic-ray energy spectrum, and n_{O} is the gas density of O atoms. The expression for $d\mathrm{B}/dt$ is readily adapted to include production from other collision pairs (see Duncan et al. 1992).

If the cosmic rays and the interstellar gas have a halo composition, Li production is dominated by α-on-α fusion reactions (Steigman & Walker 1992) with

$$d\,\mathrm{Li}/dt = \langle \phi_\alpha \sigma_{\alpha\alpha}(\mathrm{Li}) \rangle n_\alpha ,$$

where n_α is independent of Galactic age because the big bang supplies the majority of the α's. Note that ^{6}Li and ^{7}Li are described by the same form for the rate equation, but with different cross sections.

The production rates depend on the cosmic ray energy spectrum. In the likely event (Prantzos et al. 1993) that production is dominated by high-energy rays ($E \gtrsim 100$ MeV nucleon^{-1}), the shape of the spectrum is irrelevant because the cross sections approach an asymptotic value at high energies. If we adopt $\phi_\alpha = 0.1\ \phi_p$, $n_a = 0.1\ n_{\mathrm{H}}$, and a halo composition for the gas, we obtain the abundance ratio

$$\frac{\mathrm{Li}}{\mathrm{B}} \simeq \frac{0.0022 + 47\langle \mathrm{O/H} \rangle}{60\langle \mathrm{O/H} \rangle} , \qquad (4)$$

where $\langle \mathrm{O/H} \rangle$ is the O/H ratio in the gas weighted by the cosmic-ray flux and averaged over the life of the halo prior to the formation of the star with an abundance O/H. The numerical values in equation (4) are taken from Duncan et al. (1992, their eq. [6]). The Li/B ratio increases when low energy CRs are introduced. The Li/B in the gas depends on the evolution of the O abundance; for example, if synthesis of O is delayed but later proceeds rapidly, Li/B in the gas will exceed the value given by equation (4) for the O abundance of the gas. For HD 84937, equation (4) gives Li/B = 4 for the O abundance derived by Gilmore et al. (1992) from ultraviolet OH lines. If the O abundance increased linearly with time prior to the formation of HD 84937, Li/B = 8 is found. High-energy CRs lead to $r = {}^7\mathrm{Li}_{\mathrm{CR}}/{}^6\mathrm{Li}_{\mathrm{CR}} = 1/4$ and then $P = {}^6\mathrm{Li}_{\mathrm{CR}}/\mathrm{B}_{\mathrm{CR}} = 4$ to 8. Admission of lower energy CRs leads to an increase of P and a slight decrease of r.

The standard scenario of B and Be production by spallation reactions between CR p (and α) and interstellar O (and C, N) nuclei does not easily account for the linear dependence of the halo Be and B abundances on the O (and Fe) abundances. If supernovae are responsible for both the cosmic rays and the O abundance of the halo gas, one expects the Be and B abundances to vary approximately as the square of the O abundance. This relation is well shown by both simple (Vangioni-Flam et al. 1990; Ryan et al. 1992) and sophisticated (Prantzos et al. 1993) models of the growth of spallation products in the halo. The sophisticated model just fits the observed Be and B versus O trends within the observational uncertainties, but the predicted slope is not a good fit to the well determined slope of the Be abundances (Gilmore et al. 1992).

In view of the good fit of the Be abundances to a linear trend with O, it is of interest to consider here alternative models for Be and B production that lead more directly to a linear dependence and to assess the impact of these alternatives on the ^{6}Li production accompanying that of Be and B. Three proposals have been made that appear to give the desired linear relation.

First, Feltzing & Gustafsson (1993) propose that spallation occurs primarily in the immediate vicinity of the supernovae that provide the cosmic rays. If the vicinity has been contaminated with oxygen from local supernovae, the Be and B yields will scale with the oxygen abundance. This scheme should be applicable to the (competing) scenarios for the formation of globular clusters (Lin & Murray 1991; Brown, Burkert, & Truran 1991) in which protocluster gas is self-enriched by supernovae. For example, in Brown et al.'s scheme, a first generation of stars enriches the gas which later forms the presently observed stellar generation. Supernovae from this second generation expel the residual gas from the cluster. Spallation occurring before the gas is expelled may lead to Be and B enrichment of the gas such that the stars and the expelled gas contain Be and B.

Second, a linear dependence of Be and B on O would follow if the primary production path were from reactions between cosmic ray O (and C, N, ...) and "interstellar" p (and α)—see

Duncan et al. (1992). This path is of minor importance in the Galactic disk because it leads to high-energy Be and B nuclei that are partially destroyed in the collisions that thermalize the nuclei. On the other hand, collisions between CR protons and interstellar O nuclei lead to low-energy Be and B nuclei that are thermalized without great losses. To the extent that the cosmic rays reflected the composition of either the supernovae or gas enriched locally by supernovae, the reactions between O (in the CRs) and local or interstellar protons may have been dominant in the early Galaxy and then the linear relation between Be (and B) and O follows very naturally. Obviously, there is such a similarity between this and the proposal by Feltzing and Gustafsson that they might be considered as variants of a single proposal.

Third, if the dominant source of cosmic rays in the early Galaxy were external to the proto-Galaxy, spallation yields of Be and B in the halo would depend on the O abundance and, hence, Be and B depend linearly on the O abundance.

The ratio of the yields of ^{6}Li and ^{7}Li to B and Be depends on the relative contributions of the p or α on CNO spallation reactions to the α-on-α fusion reactions. In the limit that the former are dominant, Li/B $\simeq 0.8$ and ^{6}Li/^{7}Li $\simeq 0.6$ at high energies, but these ratios are only weakly dependent on the cosmic ray energy unless the low energies of the reaction thresholds are sampled. These limiting values are not, as we show below, easily reconciled with our detection of ^{6}Li in HD 84937.

The total neglect of the α-on-α reactions implied by these limiting values is not necessarily demanded by any one of the three proposals just sketched. The key issue is the presence of α's in the cosmic rays because it is reasonable to suppose that the α's are abundant in the gas comprising the targets for the cosmic rays. Spallation reactions between cosmic rays and ejecta from deep in the supernova (i.e., He-poor) are surely unimportant because, although He-poor ejecta will be present, it is likely that the accelerating shocks provided by a supernova will not accelerate its own He-poor ejecta, but gas shed earlier by a stellar wind and other gas in the vicinity. Much of the accelerated gas will contain a normal or even a higher abundance of α's. Thus it is likely that the first two of the three above proposals allow for a contribution from the α-on-α fusion reactions, but it is not easy at present to quantify the latter contribution. The third more speculative proposal would also probably provide α's in the external cosmic rays; for example, if the mechanisms of acceleration involve pre-galactic sources operating on primordial gas, the α/proton ratio will be approximately the usual ratio and α-on-α fusion reactions will occur in the early Galaxy even before oxygen is synthesized by halo supernovae.

4.2. ^{6}Li *and HD 84937*

Now we return to HD 84937 and the origin of the ^{6}Li detected by us. The key question is surely the following: was the ^{6}Li synthesized by CRs or is it the fruit of a nonstandard big bang? In order to answer this question we use equation (3)

$$^6\mathrm{Li}_{\mathrm{BB}} = \frac{R\,\mathrm{Li}}{D_6} - P\,\mathrm{B}_{\mathrm{CR}}\,, \qquad (5)$$

where Li is the observed total Li abundance, $\mathrm{B}_{\mathrm{CR}} = 1.3^{+1.7}_{-0.5}$ is inferred from the observations of B in HD 19445 and HD 140283 (Duncan et al. 1992), P was estimated above, and D_6 must be obtained from models of subdwarfs.

Before applying equation (5), we note that constraints may be set on the ^{6}Li abundance of the protogalactic and halo gas (here, $^6\mathrm{Li}_{\mathrm{BB}}$) independently of the values derived from measurements of the ratio $R = {}^6$Li/Li in stars: the ^{6}Li abundance of the current interstellar medium (and the Sun) and an estimate of the astration achieved by the Galaxy may be combined to give the halo ^{6}Li abundance. The ^{6}Li abundance of the initial solar system, as provided by carbonaceous chondrites, is ^{6}Li = 150 (Anders & Grevesse 1989). Lemoine et al. (1993) measured the ^{6}Li/^{7}Li ratio in the interstellar medium towards ρ Oph A and found it equal to the solar value. Predictions of the yields from the CR spallation and α-on-α fusion reactions show that these reactions account satisfactorily for the current ^{6}Li/Be ratio; ^{7}Li is produced primarily by stars. The agreement between the predicted and observed ^{6}Li/Be ratio suggests that most of the ^{6}Li has been synthesized in the disk by CRs. We suppose that less than about 30% of the local ^{6}Li atoms are survivors from the early Galaxy: say $^6\mathrm{Li}'_0 < 50$ where $^6\mathrm{Li}'_0$ refers to the surviving atoms where the initial abundance in the early Galaxy was $^6\mathrm{Li}_0$. To correct $^6\mathrm{Li}'_0$ to $^6\mathrm{Li}_0$, we draw on discussions of the astration of deuterium from the big bang. The galactic histories of D and $^6\mathrm{Li}_0$ must be very similar. Boesgaard & Steigman (1985) review the theoretical predictions for astration of D and suggest that the local present D/H ratio requires a correction by a factor of 2 to 10 in order to obtain the primordial ratio. Application of their suggestion to $^6\mathrm{Li}'_0$ gives $^6\mathrm{Li}_0 <$ 500. Since the predictions of D astration generally appear to favor a factor closer to 2 than 10, $^6\mathrm{Li}_0$ may be closer to 100 than 500. A correction for astration may be applied to the local ^{7}Li abundance, but here the additional uncertainty in estimating the stellar production of ^{7}Li weakens the arguement. In the conversion of the measured R to $^6\mathrm{Li}_{\mathrm{BB}}$ via equation (5), we take D_6 from two sets of models: (i) Depletion factors are taken from Pinsonneault, Deliyannis, & Demarque (1992, hereafter PDD) for standard (nonrotating) stars—see their Table 3B; (ii) depletion factors are taken from the same reference for rotating stars.

4.2.1. Li *Depletion in Standard (Nonrotating) Models for the* Li *Isotopes*

Depletion of Li in standard models of main-sequence stars occurs prior to the main sequence and, hence, is independent of age at a given mass, but increases with decreasing mass and decreases with metallicity. (For low masses, $M < 0.67\ M_\odot$, additional depletion occurs on the main sequence.) "Standard" also means that gravitational settling of Li is ignored. The predicted D_7 and D_6 are, of course, sensitive to the adoptive mixing length, opacities, etc. We shall not explore the sensitivity of D_7 and D_6 to the various effects and parameters, but note that the models represented in PDD's Table 3B and associated tables do account very satisfactorily for the Li plateau. D_7 determines the effective contribution of the CRs to the Li plateau. We estimate the mass of HD 84937 from Bergbusch & VandenBerg's (1992) isochrones for [O/Fe] = 0.75 and $Y = 0.235$. For the atmospheric parameters of HD 84937, we find $M = 0.78\ M_\odot$ at an age of 16 Gyr and $0.80\ M_\odot$ at an age of 14 Gyr. The minimum mass of $M = 0.72\ M_\odot$ occurs when HD 84937 is placed on the main sequence, but this possibility appears excluded by the spectroscopic estimate of the surface gravity. Inspection of Pinsonneault et al.'s Table 3B suggests the $D_6 = 0.7$ $(+0.1, -0.2)$ and $D_7 \simeq 1.0$ for $M = 0.80 \pm 0.02\ M_\odot$. (Gravitational settling of Li atoms increases the atmospheric ^{6}Li/^{7}Li ratio [Deliyannis 1990]. The equivalent D_6 is slightly smaller than in the standard models.)

On substitution of the observed ratio, $R = 0.05 \pm 0.02$, $D_6 = 0.7$ $(+0.1, -0.2)$, Li = 130, $P = 6 \pm 2$, and $B = 1.3$ $(+1.7, -0.5)$, we find $^6Li_{BB} = 1$ $(+15, -20)$. The error estimates of $^6Li_{BB}$ represent maximum and minimum values from equation (5). These estimates are less than the maximum ($^6Li_0$) provided by the above from Galactic astration of ^{6}Li. Both estimates of $^6Li_{BB}$ are consistent with the prediction that standard big bangs synthesize ^{7}Li, but not ^{6}Li. However, this conclusion is dependent on the adopted value of $P = {}^6Li/B_{CR}$. As we noted above, P is greatly reduced if synthesis of Li by α-on-α reactions is suppressed: then $P = 0.3$ and $^6Li_{BB} = 9$ $(+10, -6)$ for $D_6 = 0.7$ and 32 $(+60, -20)$ for $D_6 = 0.2$, suggesting some pre-Galactic production of ^{6}Li. As we indicated above, we think it unlikely that the α-on-α reactions can be so severely suppressed and, hence, pre-Galactic ^{6}Li is most probably not demanded. We postpone to the next subsection our comments on nonzero values of $^6Li_{BB}$.

The mass of HD 19445, as estimated from Bergbusch and Vandenberg's isochrones is $m \simeq 0.67\ M_\odot$ for an age of 16 Gyr and $0.68\ M_\odot$ for an age of 14 Gyr. Inspection of PDD's Table 3B shows $D_6 \simeq 0.01$ and, hence, the absence of detectable ^{6}Li in HD 19445 is fully compatible with the presence of ^{6}Li in HD 84937 for which $D_6 \simeq 0.7$.

The Li production implied by $P = 6 \pm 2$ and depletion factors $D_6 \simeq 0.7$ and $D_7 \simeq 1$ is consistent with the flatness of the Li plateau; for example, at [Fe/H] $\simeq -1.4$, the metal-rich edge of the plateau (Deliyannis et al. 1993), equation (4) and the inferred B abundance predict a Li increase of about 5% over the Li abundance (primarily $^7Li_{BB}$) seen in much more metal-poor stars. Note D_6 at a given mass is a factor of 2 to 3 smaller in the [Fe/H] $= -1.4$ stars than for HD 84937. This increase is within the 10% observational limit for the Li plateau. If the O abundance increased linearly with time up to [Fe/H] $\simeq -1.4$, the predicted increase is doubled to nearly 10%; a less rapid increase of the O abundance leads to a larger Li contribution from the CR αs. If low-energy CRs are admitted, the increase may be larger. One may, of course, cite the flatness of the plateau as evidence that low-energy CRs were unimportant and the O abundance increased quite promptly in the early Galaxy. Since the CRs synthesize primarily ^{6}Li, careful comparison of the Li abundances of the most massive halo main-sequence (i.e., the warmest with $D_6 \simeq 1$) stars with the cooler (i.e., $D_6 \simeq 0$) stars for which ^{7}Li is not expected to be depleted should betray the magnitude of the $^6Li_{CR}$ contribution.

4.2.2. Li *Depletion in Rotating Models*

When the depletion factors predicted by the rotating models are introduced, a different conclusion is reached about the origins of the observed ^{6}Li. As PDD have shown, these models can account for the Li plateau even though the factor D_7 is much less than 1: $D_7 \simeq 0.1$ or less in contrast to $D_7 \simeq 1.0$ for the standard nonrotating models. With the mass suggested by Bergbusch and VandenBerg's tracks we find $D_7 = 0.09$, 0.04, and 0.03 for the initial angular momentum set at the three values considered by Pinsonneault et al.; increasing angular momentum leads to increased depletion of Li. D_6 is not given by PDD, but may be estimated from Deliyannis (1990): $D_6 = 0.006$ at 10 Gyr falling to 0.001 at 16 Gyr for the lowest value of the initial angular momentum, and $D_6 = 0.004$ at 10 Gyr and 0.0005 at 16 Gyr for the highest of the three values of the initial angular momentum. These same models predict a modest depletion of Be ($D_{Be} = 0.5$), but presumably only a minor depletion of the B isotopes.

The formal implication of these small values of D_6 are obvious: the initial ^{6}Li content was high. For example, $^6Li_{BB} = 800$ for $D_6 = 0.006$ and 9,000 for $D_6 = 0.0005$ and the precise values of P and B_{CR} are, of course, irrelevant. If $D_7 \cong 0.1$ the estimates of $^6Li_{BB}$ correspond to $(^6Li/^7Li)_{BB} \cong 0.7$ to 8 for the two values of D_6. These values of $^6Li_{BB}$ are in conflict with both the prediction that ^{6}Li is not synthesized by standard big bangs and the upper limit $^6Li_0$ inferred from galactic astration.

Four possible interpretations of the high values of $^6Li_{BB}$ are suggested:

1. *The rotational models are inapplicable to HD 84937 and* $^6Li_{BB} \cong 0$, *as suggested by the analysis using the standard models.* Since the models of rotating stars predict ^{7}Li to be depleted by about a factor of 10, one expects the observed Li (mostly ^{7}Li) abundances to be widely spread if some stars behave like the standard models and others like the models of rotating stars. This expectation is not confirmed by the observations that show a small spread in Li abundances Therefore, the rotational models must be rejected for HD 84937 and most other halo dwarfs.

2. $^6Li_{BB} \cong 0$, *as expected from a standard big bang, but we have underestimated the true contribution of* $^6Li_{CR}$ *and the astration of* ^{6}Li *over the Galaxy's Lifetime.* We do not explore here whether astration has been seriously underestimated. Low-energy CRs enhance the value of P. The observed B/Be ratio excludes a large flux of low-energy protons because such protons increase the predicted B/Be ratio. Moreover, the rotational models predict a depletion such that the observed B/Be ($\simeq 10$) ratio must have initially been smaller (say, B/Be $\simeq 5$) and this further restricts the need for low-energy CRs. If the low-energy CRs were also present in the gas that gave birth to the stars at the metal-rich end of the Li plateau, it is difficult to achieve the flatness of the plateau. A high abundance of $^6Li_{CR}$ and accompanying B_{CR} could be reconciled with the observations of the B/Be ratio if one were to suppose that there were another Galactic source of Be; a pre-Galactic source of large amounts of Be is excluded by the fact the observed Be abundances in subdwarfs show no evidence for a Be plateau. A Galactic (i.e., stellar) source of Be, but not B or Li, is, however, a very remote possibility.

Since Li_{CR} is synthesized by CR α's, the B/Be ratio is not an absolute limit on P as low-energy CR α's unaccompanied by CR protons may be invoked. Hence, another possibility is that the required Li atoms were synthesized by the α-on-α reactions at an early era when B and Be production was hindered by a low O abundance in the ambient gas—see equation (4). If the major fraction of the inferred $^6Li_{CR}$ (and $^7Li_{CR}$) were synthesized at an early era, the flatness of the Li plateau is assured; there remains the possibility of large variations of D_6 from star-to-star and, hence, a scatter along the plateau.

3. *Our calculations predict about correctly the CR contribution to* ^{6}Li, *and the required high initial* ^{6}Li *abundance was provided by a nonstandard big bang or a pre-Galactic change of big bang abundances.* Again, invocation of a high ^{6}Li abundance requires astration to a more severe degree than predicted in order to reduce ^{6}Li to its present level. In this scenario, the Li plateau is preserved. None of the published variants of the standard big bang models are expected to synthesize the necessary amounts of ^{6}Li during the initial phase of nucleosynthesis (Malaney 1993). There remains the possibility discussed by Dimopoulos et al. (1988) that the products of the initial phase may be replaced by other products through the

interactions between the abundance ^4He nuclei and the hadronic showers from the decay of exotic massive nonbaryonic particles that decay after the initial phase. Dimopoulos et al. show that the final products of the nucleosynthesis wrought by the p, n, and photons from the decay of a particle do not depend greatly on properties of the particle; the absolute abundances of D, ^3He, ^6Li, and ^7Li depend on a single combination of the particle's properties with a second combination fixing the degree of destruction of the initial ^4He abundance. Dimopoulos et al. emphasize that their model of post–big bang nucleosynthesis predicts a $^6Li/^7Li$ ratio $\simeq 10$. Brown & Schramm (1988) first discussed the possibility of observational verification of this prediction. Audouze & Silk (1989) discussed whether this prediction and the predicted high level of D could be reconciled with observations and the expected degree of astration in the evolution of the halo and the disk. (Destruction of ^4He after big bang nucleosynthesis might account for a "low" primordial $^4He/H$ ratio.) As noted above, our detection of ^6Li and PDD's predictions of severe destruction of ^6Li and moderate destruction of ^7Li imply an initial ratio $^6Li/^7Li \simeq 1$ to 10 and, hence, could be considered to confirm Dimopoulos et al.'s prediction. The problem remains that ^6Li abundance required to match our observation exceeds that (i.e., $^6Li_0$) inferred from Galactic astration. In short, $^6Li/^7Li \simeq 10$ is reconcilable with our observation of HD 84937 if either $D_7 \simeq 1$, but D_6 is small or Galactic astration has been seriously underestimated.

4. *The observed ^6Li was synthesized on the stellar surface by energetic protons and α's from stellar flares.* At present, this is an ad hoc proposal as there is no observational evidence for flares or magnetic fields on subdwarfs like HD 84937. PDD's models of rotating stars show that Li depletion occurs continuously over the star's life, but the major phase occurs in the first few Gyr. If flare activity were to continue into the late main-sequence phase, the rate of Li synthesis could possibly exceed the continuing slow rate of Li destruction. Maintenance of ^6Li at the observed level is energetically possible. Since the surface convection zone is very shallow, the amount of Li that has to be synthesized is small and a very small diversion of the star's luminosity to power energy particles would suffice for the synthesis of Li. If Li is synthesized on the stellar surface, the initial ^6Li cannot be inferred and arguments about astration over the Galaxy's lifetime are inapplicable.

Of course, the energetic particles do not synthesize pure ^6Li. If the energy spectrum is dominated by high-energy particles, synthesis of B and Be occurs at about the levels observed in HD 84937; this conclusion follows from our earlier discussion of ^6Li and the standard (nonrotating) models. In this limited sense, B and Be might be fruits of stellar surface nucleosynthesis. Production of B and Be is suppressed relative to ^6Li and ^7Li when the energetic particles are of lower energy, say 50 MeV nucleon^{-1}. Such lower energy α's and protons would synthesize the observed ^6Li, but little B and Be.

5. CONCLUDING REMARKS

Previous searches for ^6Li in subdwarfs have established the upper limit $^6Li/^7Li \leq 0.1$. Our spectra through a careful analysis of the 6707 Å line profile show that ^6Li is present in HD 84937 ($^6Li/Li = 0.05 \pm 0.02$), but absent from the cooler less massive star HD 19445 ($^6Li/Li < 0.02$). This difference between the two stars is consistent with predictions that the less massive star should suffer the more severe depletion of atmospheric ^6Li. We feel it is also significant that two similar stars observed under identical observations in the same observing run with spectra reduced in equivalent ways yield different results for the $^6Li/^7Li$ ratio.

Interpretation of the ^6Li content of HD 84937 is beset by the uncertainty over the predicted internal depletion of ^6Li (and ^7Li). If standard stellar (Yale) models are adopted, the presence of the ^6Li in HD 84937 is quite consistent with the predicted modest depletion of ^6Li and an initial ^6Li abundance attributed to α-on-α fusion reactions involving the cosmic rays that are invoked to account for the Be and B abundances of subdwarfs. Standard models also explain why HD 19445 has destroyed all of the essentially same ^6Li abundance. There is no need to invoke pre-Galactic synthesis of ^6Li.

This tidy picture is not redrawn when Yale models of rotating stars are adopted. These predict severe depletions of ^6Li in even HD 84937 and, hence, a much higher initial ^6Li abundance seems required. We noted that this requirement may violate limits that may be set from arguments on astration and the present ^6Li abundance of interstellar gas. We sketched four competing resolutions of the problem raised by the models of rotating stars.

This competition may be solved by additional observations of ^6Li in subdwarfs. In principle, one can set out to map the $^6Li/^7Li$ abundance as a function of stellar mass and metallicity. Observations at $[Fe/H] \gtrsim -2$ are quite possible. Unfortunately, the warm (more massive) stars of $[Fe/H] < -2$ are rare and striking progress in the field of $^6Li/^7Li$ measurements may have to wait for large telescopes equipped with high resolution spectrographs. Fortunately, additional measurements can be made now, and even a few further detections of ^6Li and firm low upper limits to the $^6Li/^7Li$ ratio would serve to challenge one or more of our four proposed interpretations.

We thank J. Silk for a very helpful conversation. P. E. N. acknowledges a research stipend from the Aarhus University Research Foundation and a travel grant from the Danish Science Research Council. This research has been supported by the National Science Foundation (grant AST91-15090) and the Robert A. Welch Foundation.

REFERENCES

Anders, E., & Grevesse, N. 1989, Geochim. Cosmochim. Acta, 53, 197
Andersen, J., Gustafsson, B., & Lambert, D. L. 1984, A&A, 136, 75
Audouze, J., & Silk, J. 1989, ApJ, 342, L5
Bard, A., Kock, A., & Kock, M. 1991, A&A, 248, 315
Bergbusch, P. A., & VandenBerg, D. A. 1992, ApJS, 81, 163
Boesgaard, A. M., & Steigman, G. 1985, ARA&A, 23, 319
Brown, J. H., Burkert, A., & Truran, J. W. 1991, ApJ, 376, 115
Brown, L., & Schramm, D. N. 1988, ApJ, 329, L103
Carney, B. W., & Latham, D. W. 1987, AJ, 93, 11
Cayrel, R. 1988, in The Impact of Very High S/N Spectroscopy on Stellar Physics, ed. G. Cayrel, de Stobel, & M. Spite (Dordrecht: Kluwer), 345
Deliyannis, C. P. 1990, Ph.D. thesis, Yale Univ.
Deliyannis, C. P., Demarque, P., & Kawaler, S. D. 1990, ApJS, 73, 21
Deliyannis, C. P., Pinsonneault, M. H., & Demarque, P. 1992, ApJS, 78, 179 (PDD)
Deliyannis, C. P., Pinsonneault, M. H., & Duncan, D. K. 1993, ApJ, in press
Dimopoulos, S., Esmailzadeh, R., Hall, L. J., & Starkman, G. D. 1988, ApJ, 330, 545
Duncan D. K., Lambert, D. L., & Lemke, M. 1992, ApJ, 401, 584
Edvardsson, B., Andersen, J., Gustafsson, B., Lambert, D. L., Nissen, P. E., & Tomkin, J. 1993, A&A, submitted
Feltzing S., & Gustafsson, B. 1993, ApJ, submitted
Gilmore, G., Gustafsson, B., Edvardsson, B., & Nissen, P. E. 1992, Nature, 357, 379
Gustafsson, B., Bell, R. A., Eriksson, K., & Nordlund, Å. 1975, A&A, 42, 40
Holweger, H., & Müller, E. A. 1974, Solar Phys., 39, 19

Kurucz, R. L. 1989, private communication
Kurucz, R. L., & Peytremann, E. 1975, Smithsonian Astrophys. Obs., Spec. Rep. 362
Lemoine, M., Ferlet, R., Vidal-Madjar, A., Emerich, C., & Bertin, P. 1993, in Nuclei in the Cosmos, ed. F. Käppeler (Dordrecht: Kluwer), in press
Lin, D. N. C., & Murray, S. D. 1991, in The Formation and Evolution of Star Clusters, ed. K. Janes (ASP Conf. Ser., 13), 55
Magain, P. 1987, A&A, 181, 323
———. 1989, A&A, 209, 211
Malaney, R. A. 1993, in Nuclei in the Cosmos, ed. F. Käppeler (Dordrecht: Kluwer), in press
Maurice, E., Spite, F., & Spite, M. 1984, A&A, 132, 278
Nissen, P. E., Edvardsson, B., Gustafsson, B., & Gilmore, G. 1993, in preparation
O'Brian, T. R., Wickliffe, M. E., Lawler, J. G., Whaling, W., & Brault, J. W. 1991, J. Opt. Soc. Am., 8, 1185
Palmer, B. A., & Engleman, R., Jr. 1983, Los Alamos Sci. Lab. Rep. LA-9615
Pilachowski, C. A., Hobbs, L. M., & De Young, D. S. 1989, ApJ, 345, L39
Pinsonneault, M. H., Deliyannis, C. P., & Demarque, P. 1992, ApJS, 78, 179
Prantzos, N., Cassé, M., & Vangioni-Flam, E. 1993, ApJ, 403, 630
Risberg, G. 1968, Ark. Fys., 37, 231
Ryan, S., Norris, J. E., Bessell, M. S., & Deliyannis, C. P. 1992, ApJ, 388, 184
Schuster, W., & Nissen, P. E. 1989, A&A, 222, 69
Spite, F., & Spite, M. 1982, A&A, 115, 357
Steigman, G., & Walker, T. P., 1992, ApJ, 385, L13
Sugar, J., & Corliss, C. 1979, J. Phys. Chem. Ref. Data, 8, 865
VandenBerg, D. A., & Bell, R. A. 1985, ApJS, 58, 561
Vangioni-Flam, E., Cassé, M., Audouze, J., & Oberto, Y. 1990, ApJ, 364, 568
Wagman, N. E. 1937, Univ. Pittsburgh Bull., 34, 1